A nonlinear model for stage-structured population dynamics with nonlocal density-dependent regulation: an application to the fall armyworm moth

Gianni Gilioli[a], Pierluigi Colli[b], Michele Colturato[b], Paola Gervasio[c], Giorgio Sperandio[a]

[a] *DMMT, Università degli Studi di Brescia, viale Europa, 11, 25121 Brescia, Italy*
[b] *Dipartimento di Matematica, Università degli Studi di Pavia, via Ferrata 5, 27100 Pavia, Italy*
[c] *DICATAM, Università degli Studi di Brescia, via Branze 38, 25123 Brescia, Italy*

Abstract

The assessment and the management of the risks linked to insect pests can be supported by the use of physiologically-based demographic models. These models are useful in population ecology to simulate the dynamics of stage-structured populations, by means of functions (e.g., development, mortality and fecundity rate functions) realistically representing the nonlinear individuals physiological responses to environmental forcing variables. Since density-dependent responses are important regulating factors in population dynamics, we propose a nonlinear physiologically-based Kolmogorov model describing the dynamics of a stage-structured population in which a time-dependent mortality rate is coupled with a nonlocal density-dependent term. We prove existence and uniqueness of the solution for this resulting highly nonlinear partial differential equation. Then, the equation is discretized by finite volumes in space and semi-implicit backward Euler scheme in time. The model is applied for simulating the population dynamics of the fall armyworm moth (*Spodoptera frugiperda*), a highly invasive pest threatening agriculture worldwide.

Keywords: Physiologically-based models, Pest management, Invasive species, Solvability of nonlinear Kolmogorov equations, Numerical simulation, *Spodoptera frugiperda*.

1. Introduction

Insect pests represent an important threat for agriculture and environment and pose serious issues linked to human health (Charles and Dukes (2014), Mazza et al. (2014), Paini et al. (2016)). Among the most dangerous pests, the

*Corresponding author: Michele Colturato E-mail: michele.colturato@unibs.it

fall armyworm *Spodoptera frugiperda* (Lepidoptera: Noctuidae) represents one of the main threats for agriculture worldwide (Day et al. (2017), Early et al. (2018)). The species is known for its great migratory capacity that facilitates the spread of the species along wide areas (Kumela et al. (2019)). It feeds on more than 180 host plant species including economic valuable crops such as maize, sorghum, rice and millets (Hogg et al. (1982), Oeh et al. (2001), Murúa and Virla (2004), Busato et al. (2005), Milano et al. (2008), Baudron et al. (2019), Wang et al. (2020)). The species is native to the tropical and sub-tropical areas of South and North America. Since 2016, it has been reported in the African continent (Nigeria, Sao Tomé, Benin and Togo) where it became invasive (Goergen et al. (2016), FAO (2018)). More recently, the species has been reported in India (Ganiger et al. (2018)), Myanmar (FAO (2019c)), Sri Lanka (FAO (2019d)), China (FAO (2019b)), Bangladesh (FAO (2019a)), Thailand (IPPC (2018)) and Korea Republic (IPPC (2019)).

The high migratory capacity of the species and the risks to import infested plant products from countries with established population of *S. frugiperda* raise concerns for the potential introduction and establishment of the species in Europe (Early et al. (2018), EFSA PLH Panel (2018a)). Various modelling approaches have been applied for the assessment and the management of the risks linked to *S. frugiperda* (Farias et al. (2008), Valdez-Torres et al. (2012), Rios et al. (2014a), Rios et al. (2014b), Prasanna et al. (2018), Early et al. (2018), EFSA PLH Panel (2018b), Garcia et al. (2019), Liu et al. (2020), Wang et al. (2020), FAO (2020)). Physiologically-Based Demographic Models (PBDMs) are particularly useful to investigate the population dynamics of stage-structured populations (Gurtin and Maccamy (1974), Gyori (1990), Gyllenberg and Hanski (1992), Diekmann et al. (2001), Allen (2009), Ponosov et al. (2020)), accounting for the realistic representation of pests' physiological responses driven by environmental variables (Barfield et al. (1978), Gutierrez (1996), Garcia et al. (2019)) at different spatial (from local to regional) and temporal (short to mid-long terms) levels (Di Cola et al. (1990), Gilioli et al. (2016), Rossi et al. (2019), Pasquali et al. (2020)).

In the present contribution we present a PBDM based on the Kolmogorov equation describing the population dynamics of the *S. frugiperda*. To our knowledge, this is the first PBDM describing the population dynamics of the species. In PBDMs, the physiological responses of individuals to environmental drivers are commonly modeled through functions (i.e., development, mortality and fertility rate functions). The model presented here takes into account the nonlinear stage-specific responses of individuals to air temperature (Gutierrez (1996), Gilioli and Pasquali (2007), Regniere et al. (2012), Ponti et al. (2015)), and the effects of stochasticity on the development process of the individuals (Dautray and Lions (1988), Cushing (1992), Dautray and Lions (1992), Huffaker and Gutierrez (1999), Batchelder et al. (2002)).

As already pointed out by Gurtin and Maccamy (1974) and Diekmann et al. (2001), there are some implicit difficulties linked to using temperature as the only driver ruling the dynamics of a population. The main shortcoming is represented by the fact that the solution of the model is unbounded and thus

a population might potentially grow indefinitely depending on the persistence over time of favorable environmental conditions. Since the population growth is ruled not only by abiotic drivers (e.g. temperature, presence and availability of resources etc.) but also by biotic drivers (e.g. competition for resources and the effects of crowding) acting as density-dependent regulating factors, an indefinite population growth is biologically unrealistic (Sinclair and Pech (1996), Tamburini et al. (2013)). In particular, the population dynamics of several insect species is regulated also by density-dependent factors acting on the survival of the species (Deangelis et al. (1980), Clother and Brindley (2000)). This is also the case of *S. frugiperda*. Indeed, the species is known for the role of density-dependent factors, including larval cannibalistic behavior, in ruling the species' overall population dynamics (Barfield et al. (1978), Andow et al. (2015), Varella et al. (2015), Garcia et al. (2018)).

In order to provide a realistic description of the population dynamics of the species under investigation, we consider a Kolmogorov equation perturbed by a temperature-dependent mortality rate coupled with a nonlinear and nonlocal density-dependent term. Many stage-structured population models with density-dependent mortality terms and nonlocal factors have been proposed in the last decades (let us cite, withouth any sake of completeness, e.g., Gyori (1990), Gyllenberg and Hanski (1992), Diekmann et al. (2001), Allen (2009) Robertson et al. (2018)). However, on the basis of our knowledge, the Kolmogorov equation with a nonlinear and nonlocal density-dependent mortality term has not yet been adressed nor has its mathematical analysis been discussed.

The Kolmogorov equation with nonlinear and nonlocal density-dependent mortality term is highly nonlinear and faithfully embody three crucial biological aspects:

1. the simulation of the dynamics of a stage-structured population;
2. the representation of the stage-specific and nonlinear response of individuals to environmental drivers (i.e., air temperature);
3. the introduction of a density dependent control factor influencing the population dynamics of the species;

Let us stress that some existing models can be recovered as special cases of the model considered in this paper (a detailed comparison can ben found in Section 2).

The paper is organized as follows. Section 2 is devoted to the derivation of the model. In Section 3 we provide the numerical discretization of the partial differential equation under study by approximating the system by Finite Volumes in space and by backward Euler method in time. In order to support with empirical evidence the introduction of the density-dependent mortality term, in Section 4 we apply the model to a case study by describing the population dynamics of the fall armyworm *Spodoptera frugiperda* and show that this new approach plays a crucial role in the description of the population dynamics. Numerical results are shown in Section 5, while in Section 6 we suggest future perspectives. Finally, the Appendix is devoted to the rigorous mathematical

analysis of the model: we prove the existence of strong solutions as well as uniqueness and continuous dependence on the initial data.

2. Model derivation

The fall armyworm *Spodoptera frugiperda* can be considered as a stage structured population (eggs, larvae, pupae and adults) with discontinuous stage structure (see, e.g., Kelpin et al. (2000), Buffoni and Cappelletti (2000), Abia et al. (2004), Angulo and López-Marcos (2004), Buffoni et al. (2004), Buffoni and Pasquali (2007)). The individual growth in a single stage is described by the physiological age $x \in [0,1]$ evolving along time $t \in [0,T]$, with $T > 0$. We denote by

$$\varphi^s(t,x)\ dx$$

the average number of individuals at stage $s = 1, \dots, \mathcal{S}$, at time t with physiological age between x and $x + dx$, where dx indicates an infinitesimal variation of age. The strictly positive value $\mathcal{S} \in \mathbb{N}$ stands for the total number of growth stages: stages from 1 to $\mathcal{S}-1$ are the immature ones (e.g., eggs, larvae, pupae) while stage $\mathcal{S}$ is the reproductive one.

The seminal von Foerster equation describes the population dynamic at stage s as

$$\partial_t \varphi^s(t,x) + \partial_x \varphi^s(t,x) = -M^s \varphi^s(t,x), \qquad (t,x) \in (0,T) \times (0,1), \tag{1}$$

with boundary condition

$$\varphi^s(t,0) = \int_0^1 G^s(y)\varphi^s(t,y)\ dy, \tag{2}$$

and initial condition

$$\varphi^s(0,x) = \varphi_0^s(x), \tag{3}$$

where M^s and G^s denote the stage-specific mortality and fecundity rate, respectively, while the nonnegative function φ_0^s represents the initial abundance of each stage. In the last decades, several authors consider the von Foerster equation, suitably modified both by the introduction of time-dependent rate functions and density-dependent mortality term. We refer, e.g., to Gyori (1990), Gyllenberg and Hanski (1992), Diekmann et al. (2001) , Allen (2009), Robertson et al. (2018).

Since the development rate among individuals may depend on environmental conditions, food, assimilation and genetic characteristics, Kolmogorov adopted a stochastic approach and modified the von Foerster equation (1)–(3) by taking into account the stage-specific development rate S^s, the diffusion parameters b^s, and by replacing the term $\partial_x \varphi^s(t,x)$ with $\partial_x H^s(t,x)$, where

$$H^s(t,x) = S^s \varphi^s(t,x) - b^s \partial_x \varphi^s(t,x). \tag{4}$$

The so-called forward Kolmogorov equation is derived from the balance equation for the density function $\varphi^s(t,x)$, it is an advection-diffusion equation with elimination, namely

$$\partial_t \varphi^s(t,x) + \partial_x \Big(S^s \varphi^s(t,x) - b^s \partial_x \varphi^s(t,x) \Big) = -M^s \varphi^s(t,x), \tag{5}$$

$$\Big(S^s \varphi^s(t,x) - b^s \ \partial_x \varphi^s(t,x) \Big)_{x=0} = F^s \int_0^1 G^s(y) \varphi^s(t,y) \ dy, \tag{6}$$

$$\Big(- b^s \ \partial_x \varphi^s(t,x) \Big)_{x=1} = 0, \tag{7}$$

$$\varphi^s(0,x) = \varphi_0^s(x). \tag{8}$$

The previous system (5)–(8) can be also interpreted as a one-dimensional Fokker-Planck equation. Denoting by F^s a stage-specific positive parameter, the boundary condition (6) models the reproduction process as an input condition at the beginning of the stage, i.e., at $x = 0$. On the other hand, the boundary condition (7) states that $H^s(t,x)$ equals the number of individuals at the end of the stage itself, i.e., at $x = 1$. Finally, (8) prescribes the initial conditions of the system.

The system (5)–(8) has been widely employed in literature: we refer, e.g., to Lee et al. (1976), Plant and Wilson (1986), Bergh and Getz (1988), Iannelli (1994). Let also cite Mazzocchi et al. (2006), where an individual-based model of copepod populations is considered, and Buffoni and Pasquali (2010), where the stage structured framework of (5)–(8) is applied to describe the stage structured dynamics of a copepod population. In particular, Buffoni and Pasquali (2010) considers the following system: for $s = 1, \ldots, \mathcal{S}$

$$\partial_t \varphi^s(t,x) + \partial_x \Big(S^s \varphi^s(t,x) - b^s \partial_x \varphi^s(t,x) \Big) = -M^s \varphi^s(t,x), \tag{9}$$

$$\Big(S^s \varphi^s(t,x) - b^s \ \partial_x \varphi^s(t,x) \Big)_{x=0} = \mathcal{F}^s(t), \tag{10}$$

$$\Big(- b^s \ \partial_x \varphi^s(t,x) \Big)_{x=1} = 0, \tag{11}$$

$$\varphi^s(0,x) = \varphi_0^s(x), \tag{12}$$

where the terms

$$\mathcal{F}^1(t) \ = \ F \int_0^1 G(y) \varphi^{\mathcal{S}}(t,y) \ dy, \tag{13}$$

$$\mathcal{F}^s(t) \ = \ S^{s-1} \varphi^{s-1}(t,1), \qquad s = 2, \ldots, \mathcal{S}, \tag{14}$$

represent the input flux into stage s.

Since the mortality rate M^s of several insects species is related to the abundance of individuals themselves, in the line of Gyori (1990), Diekmann et al.

(2001) we consider a time-dependent mortality rate $M^s:\ [0,T]\mapsto[0,1]$ and the nonlocal and nonlinear density-dependent function

$$\mathcal{M}^s(t)=M^s(t)\left(1+a^s\left(\int_0^1\varphi^s(t,y)\ dy\right)^2\right)^{d^s},\qquad a^s,d^s\in(0,+\infty),\tag{15}$$

which will yield the nonlinear reaction term in the model. We observe that the integral term appearing on the right hand side of (15) represents the abundance of individuals at stage s at time t, namely

$$N^s(t)=\int_0^1\varphi^s(t,y)\ dy.$$

By replacing M^s in (9) with the density-dependent mortality term $\mathcal{M}^s$, we are led to

$$\partial_t\varphi^s(t,x)+\partial_x\Big(S^s\varphi^s(t,x)-b^s\partial_x\varphi^s(t,x)\Big)=-\varphi^s(t,x)\mathcal{M}^s(t),\tag{16}$$

for $s=1,\dots,\mathcal{S}$. Finally, we replace the classical development and reproduction rates appearing in (9)–(12) with time-dependent ones, i.e., S^s, F^s: $[0,T]\mapsto[0,1]$. Then, from (16) and (6)–(8) we obtain the *Kolmogorov equation with nonlinear and nonlocal density-dependent mortality term*, which is

$$\partial_t\varphi^s(t,x)+\ \partial_x\Big(S^s(t)\varphi^s(t,x)-b^s\partial_x\varphi^s(t,x)\Big)=-\varphi^s(t,x)\mathcal{M}^s(t),\tag{17}$$

$$\Big(S^s(t)\varphi^s(t,x)-b^s\ \partial_x\varphi^s(t,x)\Big)_{x=0}=\mathcal{F}^s(t),\tag{18}$$

$$\Big(-b^s\ \partial_x\varphi^s(t,x)\Big)_{x=1}=0,\tag{19}$$

$$\varphi^s(0,x)=\varphi_0^s(x),\tag{20}$$

where

$$\mathcal{F}^1(t)\ =\ F(t)\int_0^1 G(y)\varphi^{\mathcal{S}}(t,y)\ dy,\tag{21}$$

$$\mathcal{F}^s(t)\ =\ S^{s-1}(t)\varphi^{s-1}(t,1),\qquad s=2,\dots,\mathcal{S}.\tag{22}$$

Let us stress that some existing models can be recovered as special cases of (17)–(20): the classical Kolmogorov equation (see (5)–(8)) is obtained by setting $a^s=0$ in (15); a class of von-Foerster equations perturbed by a nonlinear and nonlocal density dependent term is obtained by choosing $a^s\neq0$ and $b^s=0$ in (15). The von Foester equation considered in Gyori (1990) can be obtained as particular case by choosing $a^s=1$, $b^s=0$ and $d^s=1$ in (15).

In Section 7 we prove that the model (17)–(20) admits a unique solutions that depends continuously on the data (the latter property ensures that if the data of the problem are slightly perturbed, e.g., by measurement uncertainty, then the solution provided by the model is slightly affected by the perturbation on the data).

Although of fundamental importance, the rigorous mathematical analysis of the model (17)–(20) is moved to Section 7 in order to make the paper more readable to non mathematicians.

3. Numerical discretization

3.1. Discretization of the system (17)–(20) *for a single stage*

We approximate system (17)–(20) by Finite Volumes in space and the backward Euler method in time (see, e.g., Quarteroni (2017)). Given a positive integer N_x we set $\Delta x = \frac{1}{N_x}$, we define the nodes

$$x_k = (k - 0.5)\Delta x \quad \text{for } k = 1, \dots, N_x, \tag{23}$$

and we consider the partition of the interval $[0, 1]$ into the control volumes

$$I_k = \left[x_k - \tfrac{\Delta x}{2}, x_k + \tfrac{\Delta x}{2}\right], \quad \text{for } k = 1, \dots, N_x. \tag{24}$$

Then, for $k = 1, \dots, N_x$, we denote by $x_{k-\frac{1}{2}}$ and $x_{k+\frac{1}{2}}$ the left and right endpoints, respectively, of the volume I_k (see Fig. 1).

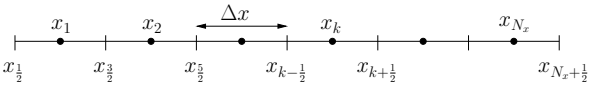

Figure 1: The nodes and the control volumes in the interval $[0, 1]$

For any $t \in (0, T)$, we restrict the differential equation (59) on each control volume I_k and we integrate it by parts, we have

$$\begin{aligned} &\partial_t \int_{I_k} \varphi(t,x)dx + H(t,x)|_{x=x_{k+\frac{1}{2}}} - H(t,x)|_{x=x_{k-\frac{1}{2}}} + \\ &\quad M(t)\left(1 + a\left(\int_0^1 \varphi(t,x)dx\right)^2\right)^d \int_{I_k} \varphi(t,x)dx = 0, \end{aligned} \tag{25}$$

where $H(t, x)$ has been defined in (4).

Then, for any $t \in (0, T)$ let $\varphi_{\Delta x}(t, x)$ a function that is constant with respect to the x variable on each control volume I_k and we set

$$\varphi_k(t) = \varphi_{\Delta x}(t, \cdot)|_{I_k} \quad \text{for } k = 1, \dots, N_x \text{ and } \boldsymbol{\varphi}(t) = \begin{bmatrix} \varphi_1(t) \\ \varphi_2(t) \\ \vdots \\ \varphi_{N_x}(t) \end{bmatrix}. \tag{26}$$

$\varphi_k(t)$ is an approximation of the average on I_k of the unknown function $\varphi(t, x)$.

From now on, for sake of clearness we set

$$\mathcal{M}_{\Delta x}(\boldsymbol{\varphi}(t)) = M(t)\left(1 + a\left(\int_0^1 \varphi_{\Delta x}(t,x)dx\right)^2\right)^d, \tag{27}$$

and we notice that

$$\int_0^1 \varphi_{\Delta x}(t,x)dx = \Delta x \sum_{k=1}^{N_x} \varphi_k(t). \tag{28}$$

Let us denote by $|I_k|$ the measure of the $k-$th control volume I_k. The finite volumes discretization of (25) reads

$$|I_k|\frac{d\varphi_k(t)}{dt} + H_k^+(t) - H_k^-(t) + \mathcal{M}_{\Delta x}(\boldsymbol{\varphi}(t))|I_k|\varphi_k(t) = 0, \tag{29}$$

where $H_k^-(t)$ and $H_k^+(t)$ are suitable approximations of $H(t,x)|_{x=x_{k-\frac{1}{2}}}$ and $H(t,x)|_{x=x_{k+\frac{1}{2}}}$, respectively, obtained by applying second-order (with respect to Δx) central finite difference schemes (see, e.g., LeVeque (2002)).

More precisely, after setting

$$\mathcal{G}_{\Delta x}(\boldsymbol{\varphi}(t)) = \Delta x \sum_{k=1}^{N_x} G(x_k)\varphi_k(t) \tag{30}$$

(in fact $\mathcal{G}_{\Delta x}(\boldsymbol{\varphi}(t))$ is the approximation of the integral $\int_0^1 G(x)\varphi(t,x)dx$ by the composite mid-point rule (see, e.g., Quarteroni et al. (2014))), and in view of both (4) and the boundary conditions (18)–(19), we have:

$$\begin{aligned}
H_1^-(t) &= F(t)\mathcal{G}_{\Delta x}(t) \\
H_k^-(t) &= S(t)\frac{\varphi_k(t)+\varphi_{k-1}(t)}{2} - b\frac{\varphi_k(t)-\varphi_{k-1}(t)}{\Delta x}, \qquad k = 2,\dots,N_x, \\
H_k^+(t) &= S(t)\frac{\varphi_{k+1}(t)+\varphi_k(t)}{2} - b\frac{\varphi_{k+1}(t)-\varphi_k(t)}{\Delta x}, \qquad k = 1,\dots,N_x-1, \\
H_{N_x}^+(t) &= S(t)\varphi_{N_x}(t).
\end{aligned} \tag{31}$$

By writing (29) for any $k = 1,\dots,N_x$ and by recalling that $|I_k| = \Delta x$ for $k = 1,\dots,N_x$, the semi-discrete approximation of the system (17)–(20) reads: given $\varphi_k(0) = \varphi_0(x_k)$ for $k = 1,\dots,N_x$, for any $t \in (0,T)$ look for the functions $\varphi_1(t),\dots,\varphi_{N_x}(t)$ such that

$$\begin{cases}
\frac{d\varphi_1}{dt}(t) + \left[\frac{S(t)}{2\Delta x} + \frac{b}{(\Delta x)^2} + \mathcal{M}_{\Delta x}(\boldsymbol{\varphi}(t))\right]\varphi_1(t) \\
\qquad\qquad + \left[\frac{S(t)}{2\Delta x} - \frac{b}{(\Delta x)^2}\right]\varphi_2(t) = \frac{F(t)}{\Delta x}\mathcal{G}_{\Delta x}(\boldsymbol{\varphi}(t)), \\
\frac{d\varphi_k}{dt}(t) - \left[\frac{S(t)}{2\Delta x} + \frac{b}{(\Delta x)^2}\right]\varphi_{k-1}(t) + \left[\frac{2b}{(\Delta x)^2} + \mathcal{M}_{\Delta x}(\boldsymbol{\varphi}(t))\right]\varphi_k(t) \\
\qquad\qquad + \left[\frac{S(t)}{2\Delta x} - \frac{b}{(\Delta x)^2}\right]\varphi_{k+1}(t) = 0, \quad \text{for } k = 2,\dots,N_x-1 \\
\frac{d\varphi_{N_x}}{dt}(t) - \left[\frac{S(t)}{2\Delta x} + \frac{b}{(\Delta x)^2}\right]\varphi_{N_x-1}(t) \\
\qquad\qquad + \left[\frac{S(t)}{2\Delta x} + \frac{b}{(\Delta x)^2} + \mathcal{M}_{\Delta x}(\boldsymbol{\varphi}(t))\right]\varphi_{N_x}(t) = 0.
\end{cases} \tag{32}$$

By setting

$$\boldsymbol{\varphi}^0 = \begin{bmatrix} \varphi_0(x_1) \\ \varphi_0(x_2) \\ \vdots \\ \varphi_0(x_{N_x}) \end{bmatrix}, \quad A(t) = \begin{bmatrix} \beta_1(t) & \gamma_1(t) & 0 & 0 & \cdots & 0 & 0 \\ \alpha_2(t) & \beta_2(t) & \gamma_2(t) & 0 & \cdots & 0 & 0 \\ 0 & \alpha_3(t) & \beta_3(t) & \gamma_3(t) & \cdots & 0 & 0 \\ \cdots & \cdots & \cdots & \cdots & \cdots & \cdots & \cdots \\ \cdots & \cdots & \cdots & \cdots & \cdots & \cdots & \cdots \\ 0 & 0 & 0 & 0 & \cdots & \alpha_{N_x}(t) & \beta_{N_x}(t) \end{bmatrix}, \tag{33}$$

with

$$\begin{aligned} &\beta_1(t) = \tfrac{S(t)}{2\Delta x} + \tfrac{b}{(\Delta x)^2},\ \gamma_1(t) = \tfrac{S(t)}{2\Delta x} - \tfrac{b}{(\Delta x)^2}, \\ &\alpha_k(t) = -\left(\tfrac{S(t)}{2\Delta x} + \tfrac{b}{(\Delta x)^2}\right),\ \beta_k(t) = \tfrac{2b}{(\Delta x)^2},\ \gamma_k(t) = \tfrac{S(t)}{2\Delta x} - \tfrac{b}{(\Delta x)^2}, \\ &\qquad\qquad\qquad\qquad\qquad\qquad\qquad\qquad \text{for } k = 2, \dots, N_x - 1 \\ &\alpha_{N_x}(t) = -\left(\tfrac{S(t)}{2\Delta x} + \tfrac{b}{(\Delta x)^2}\right),\ \beta_{N_x}(t) = \tfrac{S(t)}{2\Delta x} + \tfrac{b}{(\Delta x)^2}, \end{aligned}$$

and $\mathbf{e}_1 \in \mathbb{R}^{N_x \times 1}$ the array whose first entry is equal to one while all the others are equal to zero, the algebraic semidiscrete form of (32) reads

$$\begin{cases} \dfrac{d\boldsymbol{\varphi}}{dt}(t) + A(t)\boldsymbol{\varphi}(t) + \mathcal{M}_{\Delta x}(\boldsymbol{\varphi}(t))\boldsymbol{\varphi}(t) = \dfrac{F(t)}{\Delta x}\mathcal{G}_{\Delta x}(\boldsymbol{\varphi}(t))\mathbf{e}_1, & t \in (0, T) \\ \boldsymbol{\varphi}(0) = \boldsymbol{\varphi}^0. \end{cases} \tag{34}$$

In general the constant b is very small compared to the advection coefficient $S(t)$. To overcome numerical instabilities due to the finite difference approximation (31), we choose the discretization step Δx small enough, more precisely, we ask that (see LeVeque (2002))

$$\Delta x \leq \frac{2b}{\max_t |S(t)|}.$$

The full discretization of system (17)–(20) is achieved by applying the Backward Euler method to (34). To this aim let us fix a positive integer N_T, denote by $\Delta t = T/N_T$ the time discretization step, set $t^n = n\Delta t$, and denote by $\boldsymbol{\varphi}^n$ the approximation of $\boldsymbol{\varphi}(t^n)$. It reads: given $\boldsymbol{\varphi}^0$ as in (33), for $n = 1, \dots, N_T$ look for $\boldsymbol{\varphi}^n$ such that

$$\frac{\boldsymbol{\varphi}^n - \boldsymbol{\varphi}^{n-1}}{\Delta t} + A(t^n)\boldsymbol{\varphi}^n + \mathcal{M}_{\Delta x}(\boldsymbol{\varphi}^n)\boldsymbol{\varphi}^n = \frac{F(t^n)}{\Delta x}\mathcal{G}_{\Delta x}(\boldsymbol{\varphi}^n)\mathbf{e}_1. \tag{35}$$

In order to overcome the non-linearity in $(35)_1$ (and then to avoid a large computational effort at each time step t^n) we replace the term $\mathcal{M}_{\Delta x}(\boldsymbol{\varphi}^n)$ with $\mathcal{M}_{\Delta x}(\boldsymbol{\varphi}^{n-1})$, that means to take into account a delay of size Δt in the mortality function. Accordingly, even if the right hand side of (35) is linear with respect to $\boldsymbol{\varphi}^n$, we apply the same delay to it, that is we replace $\mathcal{G}_{\Delta x}(\boldsymbol{\varphi}^n)$ with $\mathcal{G}_{\Delta x}(\boldsymbol{\varphi}^{n-1})$, with the purpose to not alterate the tridiagonal pattern of the matrix $A(t)$. As a

matter of fact, solving a tridiagonal system of size N_x with the Thomas method (Quarteroni et al., 2014, Sect. 5.6) is very cheap since only $\mathcal{O}(N_x)$ floating point operations are required. On the contrary, should we consider $\mathcal{G}_{\Delta x}(\boldsymbol{\varphi}^n)$ instead of $\mathcal{G}_{\Delta x}(\boldsymbol{\varphi}^{n-1})$, the small bandwidth of the matrix $A(t^n)$ would be lost, fill-in of the matrix would occur, and the computational cost in computing $\boldsymbol{\varphi}^n$ would increase up to $\mathcal{O}(N_x^3)$ floating point operations (Quarteroni et al., 2014, Ch. 5).

Then, instead of (35) that is nonlinear, we solve the linearized problem (in fact we are applying a semi-implicit version of the Backward Euler method): given $\boldsymbol{\varphi}^0$ as in (33), for $n = 1, \ldots, N_T$ look for $\boldsymbol{\varphi}^n$ such that

$$\frac{\boldsymbol{\varphi}^n - \boldsymbol{\varphi}^{n-1}}{\Delta t} + A(t^n)\boldsymbol{\varphi}^n + \mathcal{M}_{\Delta x}(\boldsymbol{\varphi}^{n-1})\boldsymbol{\varphi}^n = \frac{F(t^n)}{\Delta x}\mathcal{G}_{\Delta x}(\boldsymbol{\varphi}^{n-1})\mathbf{e}_1. \tag{36}$$

We denote by $\tilde{\varphi}(t, x)$ the numerical approximation of the solution $\varphi(t, x)$ of (17)–(20) obtained so far. $\tilde{\varphi}(t, x)$ is a piecewise constant function in both t and x, more precisely, denoting by $\boldsymbol{\varphi}_k^n$ the $k-$th component of the array $\boldsymbol{\varphi}^n$ (for $k = 1, \ldots, N_x$), we have

$$\tilde{\varphi}(t, x) = \boldsymbol{\varphi}_k^n \quad \forall (t, x) \in [t^n, t^{n+1}) \times I_k. \tag{37}$$

By using standard arguments (see, e.g., LeVeque (2002); Quarteroni (2017)), it can be proved that $\tilde{\varphi}(t, x)$ is an approximation of $\varphi(t, x)$ that is second order accurate with respect to Δx and first-order accurate with respect to Δt, provided that both Δx and Δt are small enough.

3.2. Discretization of the multistage problem

For any stage s, we proceed as done in the previous Section. We denote by $(\boldsymbol{\varphi}^s)^n$ the fully discrete solution of the function φ^s at time t^n and, similarly, by $A^s(t^n)$ the Finite Volume matrix at stage s and time t^n, and so on for the other variables.

The approximation of the multistage system (17)–(20) by centered second-order Finite Volumes in space and semi-implicit Backward Euler method in time reads:

given $(\boldsymbol{\varphi}^1)^0, \ldots, (\boldsymbol{\varphi}^{\mathcal{S}})^0$,

for $n = 1, \ldots, N_T$, *look for* $(\boldsymbol{\varphi}^1)^n, \ldots, (\boldsymbol{\varphi}^{\mathcal{S}})^n$ *such that*

$$\frac{(\boldsymbol{\varphi}^1)^n - (\boldsymbol{\varphi}^1)^{n-1}}{\Delta t} + A^1(t^n)(\boldsymbol{\varphi}^1)^n + \mathcal{M}^1_{\Delta x}((\boldsymbol{\varphi}^1)^{n-1})(\boldsymbol{\varphi}^1)^n = \\ = \frac{F^1(t^n)}{\Delta x}\mathcal{G}_{\Delta x}((\boldsymbol{\varphi}^{\mathcal{S}})^{n-1})\mathbf{e}_1$$

for $s = 2, \ldots, \mathcal{S}$

$$\frac{(\boldsymbol{\varphi}^s)^n - (\boldsymbol{\varphi}^s)^{n-1}}{\Delta t} + A^s(t^n)(\boldsymbol{\varphi}^s)^n + \mathcal{M}^s_{\Delta x}((\boldsymbol{\varphi}^s)^{n-1})(\boldsymbol{\varphi}^s)^n = \\ = S^{s-1}(t^n)(\boldsymbol{\varphi}^{s-1})^n_{N_x}\mathbf{e}_1,$$

where we recall that super–index n and sub–index N_x in $(\boldsymbol{\varphi}^{s-1})^n_{N_x}$ denote the time–step and the finite volume, respectively.

4. Application to the case study of *Spodoptera frugiperda*

The model presented is applied for simulating the population dynamics of *S. frugiperda*. We consider the stage-structured model (17)–(20) and specify the stage-specific functions and the parameters (56)–(57) for stage $s = 1, \dots, 4$.

According to Buffoni and Pasquali (2010), we fix the diffusion coefficient $b^s = 0.001$ for every $s = 1, \dots, 4$ and assume that development, mortality and fertility rate functions M, S and F introduced in (56)–(57) depend on time only through the temperature $\vartheta(t)$, $\vartheta \in C^1([0, T])$, then we define $\tilde{S}$, $\tilde{M}$ and $\tilde{F}$ such that

$$\tilde{S}(\vartheta(t)) = S(t), \qquad \tilde{M}(\vartheta(t)) = M(t), \qquad \tilde{F}(\vartheta(t)) = F(t). \tag{38}$$

4.1. Data

The stage-specific development, mortality and fertility rate functions are estimated with the following procedure. Temperature-dependent responses of the rate functions are estimated based on data from different laboratory studies conducted in climate chambers under constant temperature conditions and collected at the individual level.

For estimating the develelopment rate function we have used data from Barfield et al. (1978), Hogg et al. (1982), Simmons (1993), Busato et al. (2005), Milano et al. (2008), Barros et al. (2010a), Ros-Dez and Saldamando-Benjumea (2011), Garcia et al. (2019).

For estimating the mortality rate function we have used data from Barfield et al. (1978), Simmons (1993), Murúa and Virla (2004), Busato et al. (2005), Milano et al. (2008) and Garcia et al. (2019).

For estimating the fertility rate function (see (48)) we have used data from Barfield et al. (1978), Pashley et al. (1995), Oeh et al. (2001), Milano et al. (2008), Barros et al. (2010b), Garcia et al. (2018) and Garcia et al. (2019), which refer to the temperature-dependent average total fecundity $[eggs \cdot days^{-1}]$, the average daily fecundity $[eggs \cdot female^{-1} \cdot days^{-1}]$ and the average duration $[days]$ of the oviposition period. Data used for estimating the oviposition profile G (see (50)) refer to the age-dependent amount of eggs laid by a female (Murúa and Virla (2004)) tested under controlled laboratory conditions.

For estimating the parameters of the density-dependent component influencing the larval mortality rate, we use time-series data related to *S. frugiperda* adult trap catches. Data collected in Irapuato (Guanajuato, Mexico) in 2015 (Salas-Araiza et al. (2018)) are used to estimate the parameters of the density-dependent mortality rate function through a calibration procedure (see Section 4.3). Then, we use a second dataset referring to time-series adult trap catches collected in Gainesville (Florida, US) in 2013 (Garcia et al. (2018)) for model validation.

Data related to *S. frugiperda* adult trap catches used for estimating the parameters of the density dependent mortality term (44) are reported in Salas-Araiza et al. (2018) and Garcia et al. (2018) referring to the areas of Irapuato (Guanajuato, Mexico) in 2015 and Gainesville (Florida, US) in 2013, respectively.

Table 1: The parameters used to model the functions $S^s(t)$ defined in (39)

	$s=1$	$s=2$	$s=3$	$s=4$
p^s	$3.47 \cdot 10^{-2}$	$5.18 \cdot 10^{-3}$	$8.81 \cdot 10^{-3}$	$5.76 \cdot 10^{-3}$
$\vartheta^s_\triangledown$	10.60	10.90	12.17	5.174
$\vartheta^s_\triangle$	34.90	37.59	40.00	40.00

Time-series of temperature data used in our model have been obtained considering daily minimum and mamixum air temperature from the NASA Power Global Meteorology, Surface Solar Energy and Climatology Data Client (https://power.larc.nasa.gov/, accessed: 15 May 2019). Hourly temperature data are then calculated using the algorithm described in Gilioli et al. (2014).

4.2. Development rate function

Since the development rate S is null for temperatures under a lower threshold $\vartheta^s_\triangledown$ and above a upper threshold $\vartheta^s_\triangle$, it is reasonable to consider the temperature-dependent development Briére rate proposed in Briere et al. (1999), namely

$$S^s(t) = \tilde{S}^s(\vartheta) = \max(p^s \vartheta(\vartheta - \vartheta^s_\triangledown)\chi(\vartheta)\sqrt{\vartheta^s_\triangle - \vartheta}, 1), \qquad s = 1, \dots, 4, \quad (39)$$

where p^s is a positive stretching parameter and χ is the characteristic function of the interval $[\vartheta^s_\triangledown, \vartheta^s_\triangle]$. The parameters p^s, $\vartheta^s_\triangledown$ and $\vartheta^s_\triangle$ are computed by the `lsqcurvefit` function of MATLAB© which finds the coefficients of (39) with the purpose to best fit the nonlinear function $\tilde{S}$ to the data (see Sec. 4.1) in the least-square sense. It is straightforward to prove that the optimum development temperature $\widehat{\vartheta}^s$ does not depend on the parameter p^s. Indeed, we have that

$$\widehat{\vartheta}^s = \frac{4\vartheta^s_\triangle + 3\vartheta^s_\triangledown + \sqrt{16{\vartheta^s_\triangle}^2 + 9{\vartheta^s_\triangledown}^2 - 16\vartheta^s_\triangle\vartheta^s_\triangledown}}{10}, \qquad s = 1, \dots, 4. \quad (40)$$

In Table 1 we list the parameters of the functions S^s, $s = 1, \dots, 4$ defined in (39), while the corresponding graphs are shown in Figure 2.

4.3. Mortality rate function

For each stage $s = 1, \dots, 4$, we define the average stage proportional mortality μ^s, modeled with a convex and continuous function, namely $\mu^s(\vartheta) = \max(\tilde{\mu}^s(\vartheta), 0)$ with

$$\tilde{\mu}^s(\vartheta) = \begin{cases} k^s, & \vartheta < \vartheta^{inf}_{k_s}, \\ A^s\vartheta^2 + B^s\vartheta + C^s, & \vartheta^{inf}_{k^s} \le \vartheta \le \vartheta^{sup}_{k^s}, \\ k^s, & \vartheta > \vartheta^{sup}_{k^s}, \end{cases} \quad , \quad (41)$$

where $k^s \in [0, 1]$ and $A^s > 0$. The coefficients A^s, B^s and C^s are obtained by linear least-square fitting to the mortality data. Then, fixing a cut-off threshold

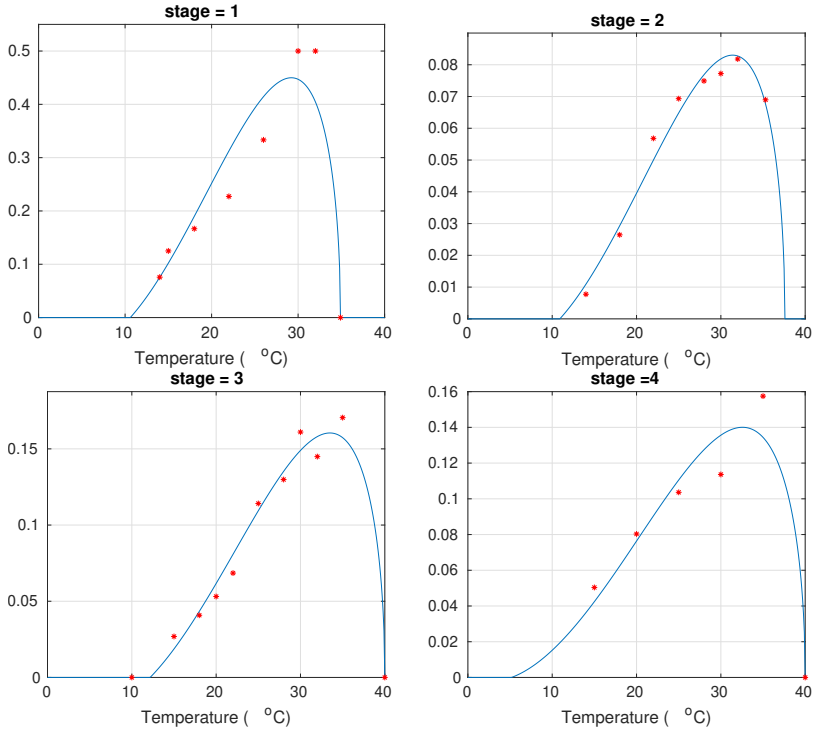

Figure 2: Development rate functions S^s, $s = 1 \ldots, 4$.

k^s, we find $\vartheta_{k^s}^{sup}$ and $\vartheta_{k^s}^{inf}$ in order to guarantee that μ^s is globally continuous. In Table 2 we list the parameters used to define μ^s, while the corresponding graphs are shown in 3. Then, we consider the function

$$m^s(\vartheta) = \begin{cases} c_{1l}^s(\vartheta - \vartheta_{k^s}^{inf})^2 + c_{2l}^s(\vartheta - \vartheta_{k^s}^{sup}) + c_{3l}^s, & \vartheta < \vartheta_{\triangledown}^s, \\ -S^s(\vartheta)\ln(1-\mu^s(\vartheta)), & \vartheta_{\triangledown}^s \leq \vartheta \leq \vartheta_{\triangle}^s, \\ c_{1r}^s(\vartheta - \vartheta_{k^s}^{sup})^2 + c_{2r}^s(\vartheta - \vartheta_{k}^{sup}) + c_{3r}^s, & \vartheta > \vartheta_{\triangle}^s, \end{cases} \tag{42}$$

where the parameters c_{il}^s and c_{ir}^s, $i = 1, 2, 3$, of the outer branches of m^s are inferred from the constraints on sign, slope and concavity of the middle branch in order to guarantee that m^s is globally C^1. According to Wagner et al. (1984), we define the mortality rate

$$M^s(t) = \tilde{M}^s(\vartheta) = \min\Big(m^s(\vartheta), 1\Big) \tag{43}$$

and list the parameters of m^s in Table 3 and the corresponding graphs in Figure 4, respectively. In order to model the larval competition and cannibalism,

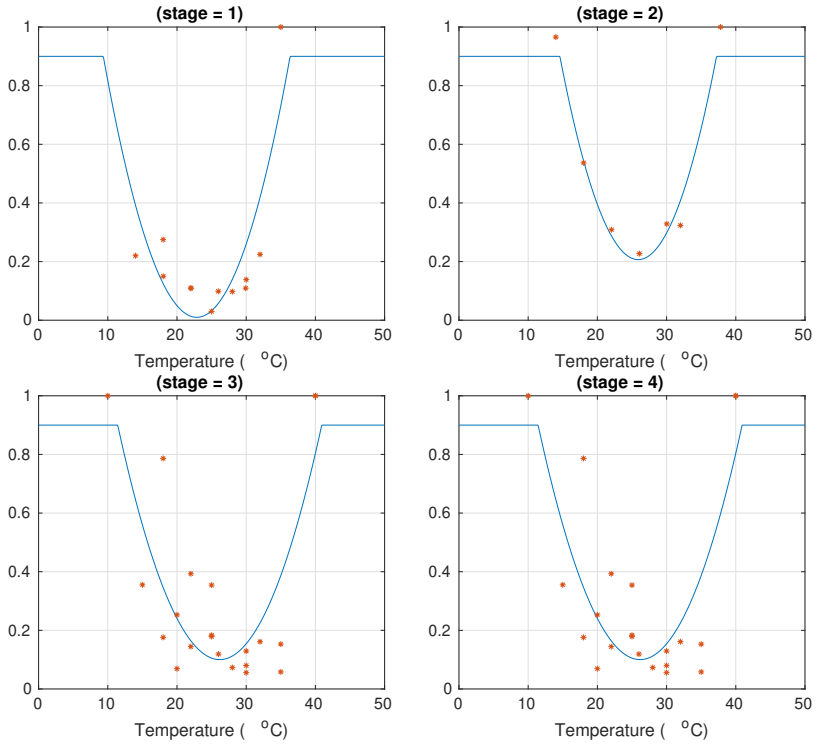

Figure 3: Average stage proportional mortality μ^s, $s = 1 \ldots, 4$.

Table 2: The parameters used to model the functions $\tilde{\mu}^s(t)$ defined in (41)

	$s=1$	$s=2$	$s=3$	$s=4$
k^s	0.9	0.9	0.9	0.9
$\vartheta_{k^s}^{sup}$	36.41	37.32	40.91	40.91
$\vartheta_{k^s}^{inf}$	9.22	14.60	11.31	11.31
A^s	$4.89 \cdot 10^{-3}$	$5.41 \cdot 10^{-3}$	$3.70 \cdot 10^{-3}$	$3.70 \cdot 10^{-3}$
B^s	$-2.23 \cdot 10^{-1}$	$-2.80 \cdot 10^{-3}$	$-1.93 \cdot 10^{-1}$	$-1.93 \cdot 10^{-1}$
C^s	2.56	3.84	2.62	2.62

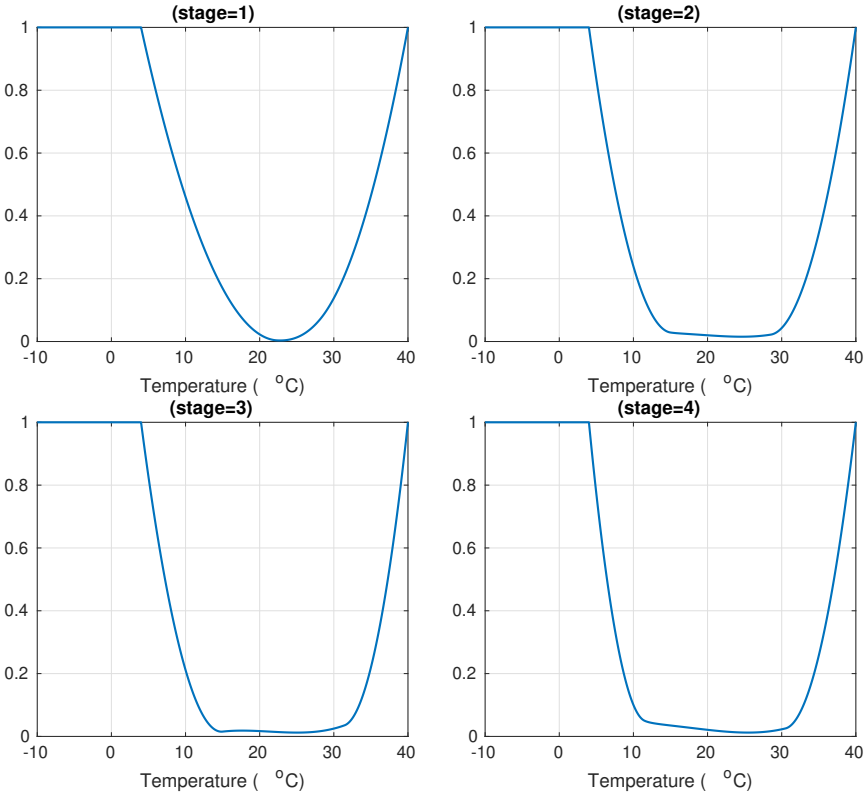

Figure 4: Mortality rate functions M^s, $s = 1 \ldots, 4$.

Table 3: The parameters used to model the functions $\tilde{\mu}^s(t)$ defined in (42)

	$s=1$	$s=2$	$s=3$	$s=4$
ϑ^s_Δ	28.08	28.52	21.61	15.78
ϑ^s_∇	22.38	15.00	15.00	15.00
c^s_{1l}	$2.88 \cdot 10^{-3}$	$7.70 \cdot 10^{-3}$	$8.4 \cdot 10^{-3}$	$1.55 \cdot 10^{-2}$
c^s_{2l}	$-1.30 \cdot 10^{-2}$	$-2.35 \cdot 10^{-1}$	$-2.49 \cdot 10^{-1}$	$-3.67 \cdot 10^{-1}$
c^s_{3l}	1.46	1.82	1.86	2.22
c^s_{1r}	$4.21 \cdot 10^{-3}$	$7.10 \cdot 10^{-3}$	$1.22 \cdot 10^{-2}$	$1.02 \cdot 10^{-2}$
c^s_{2r}	$-2.09 \cdot 10^{-1}$	$-4.01 \cdot 10^{-2}$	$-7.59 \cdot 10^{-1}$	$-6.175 \cdot 10^{-1}$
c^s_{3r}	2.61	5.59	11.84	$9.36 \cdot 10^{-1}$

following Pasquali et al. (2020), we consider a density-dependent mortality term

$$\mathcal{M}^s(t) = M^s(t)\left(1 + a^s\left(\int_0^1 \varphi^s(t,y)\ dy\right)^2\right)^{d^s}, \tag{44}$$

applied only in stage $s = 2$. The calibration procedure leads to the estimation of the density-dependent mortality term parameters a^s and d^s ($s = 2$), obtained as the minimisers of the *root mean square error*

$$RMSE(\hat{a},\hat{d}) = \sqrt{\frac{1}{n}\sum_{i=1}^{n}(N^4(t_i,\hat{a},\hat{d}) - \bar{N}_i^4)^2)}, \tag{45}$$

in which $\bar{N}_i^4$ (for $i = 1,\dots,n$) are the measured abundances of the 4th stage at certain times t_i in Irapuato (Guanajuato, Mexico), while $N^4(t_i,\hat{a},\hat{d})$ are the abundances computed with our model with a^2 and d^2 in (44) replaced by $\hat{a}$ and $\hat{d}$, respectively. The minimisers of $RMSE$ have been computed by the *interior-point method* (see, e.g., Pólik and Terlaky (2010)) implemented in the `fmincon` function of MATLAB©. The parameters obtained are

$$a^2 = 49.92 \qquad \text{and} \qquad d^2 = 0.267. \tag{46}$$

4.4. Fertility rate function

The input flux of eggs in stage $s = 1$ is defined by

$$\mathcal{F}^1(t) = \int_0^1 F(t)G(x)\varphi^4(t,x)\ dx, \tag{47}$$

where $D(t,x) = F(t)G(x)$ is the temperature- and age-dependent fertility rate function, where $F(t)$ is the temperature-dependent fertility rate and $G(x)$ is the reproductive profile which depends on adult female age. Since experimental data suggest that F is concave in a specific temperature range $[\vartheta_m^E, \vartheta_M^E]$ with a peak at the optimal temperature $\widehat{\vartheta}^E$, the temperature-dependent fertility rate is defined by the following analytic expression (see, e.g. Royer et al. (1999))

$$F(t) = \tilde{F}(\vartheta) = k^E\vartheta\chi(\vartheta)\Big(\vartheta - \vartheta_m^E\Big)\sqrt{\vartheta_M^E - \vartheta}, \qquad k^E > 0, \tag{48}$$

where χ is the characteristic function of the interval $[\vartheta_m^E, \vartheta_M^E]$. The coefficients k^E, ϑ_m^E and ϑ_M^E are computed by the `lsqcurvefit` function of MATLAB©, fitting (in the least-square sense) the nonlinear function (48) to the data. We find

$$k^E = 0.111, \qquad \vartheta_m^E = 11.442, \qquad \vartheta_M^E = 35.576. \tag{49}$$

For estimating the age-dependent fertility rate function G we refer to the data reported in Murúa and Virla (2004) which provide data that have been

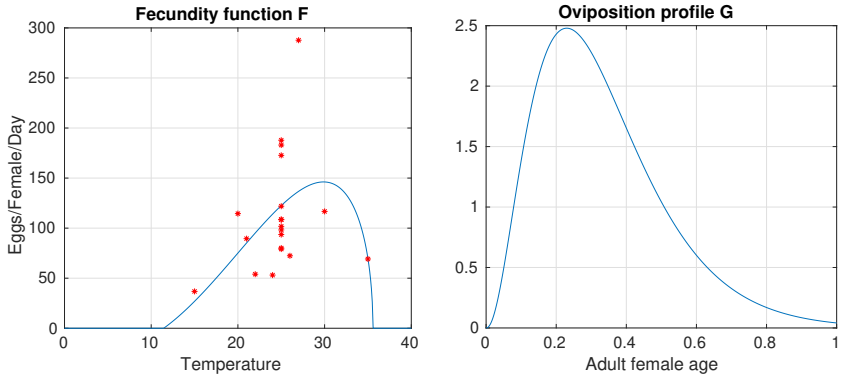

Figure 5: Functions F and G.

interpolated with the normalized Gamma distribution (see Sporleder et al. (2004)). Based on Murúa and Virla (2004), we assume that, the maximum value of eggs occurs at the optimal age $x_{opt} = 0.23$, and then declines up to a final age $x_{end} = 0.92$. Then, we consider the normalized Gamma distribution

$$G(x) = \frac{x^{\alpha-1}e^{-\beta x}}{\|x^{\alpha-1}e^{-\beta x}\|_{L^1(0,1)}}, \tag{50}$$

where α and β are positive parameters obtained in order to guarantee that the maximum age-dependent fertility rate occurs at physiological age $x_{opt} = 0.23$, i.e.,

$$x_{opt} = \frac{\alpha - 1}{\beta} = 0.23 \tag{51}$$

and that

$$\int_0^{x_{end}} x^{\alpha-1}e^{-\beta x}\, dx = \frac{99}{100}\int_0^1 x^{\alpha-1}e^{-\beta x}\, dx. \tag{52}$$

Applying (51)–(52), we find

$$\alpha = 0.318 \cdot 10^1, \qquad \beta = 0.948 \cdot 10^1. \tag{53}$$

The plots of F and G (see (48) and (50)) are shown in Figure 5.

5. Numerical results

Following the numerical model described in Section 3, we set the number of finite volumes equal to $N_x = 225$ for the stage $s = 1$ and $N_x = 100$ for the other stages. The finer discretization in the first stage is justified by the larger stretching parameters p^1 (with respect to the others p^s for $s \geq 2$; see formula (39)) which is reflected on the larger Péclet number associated with the advection-diffusion equation (see Quarteroni (2017)). We can say that the chosen discretization is sufficiently fine, in fact the relative error between this

numerical solution and that obtained by doubling the number of finite volumes in each stage is less than 10^{-4}.

The discretization time-step Δt is chosen equal to one hour, that is the frequency at which the data have been measured. This time-step is suitable to guarantee a sufficient accuracy of the numerical solution; the relative error between the solutions computed with $\Delta t = 1$ hour and $\Delta t = 1/2$ hour is less than 1%.

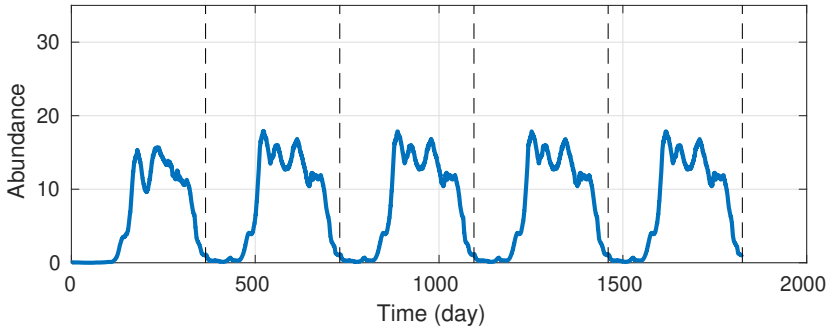

Figure 6: Numerical solution for the stage s=4 of the model implemented in the location of Irapuato (Guanajuato, Mexico) with $a^s = 49.92$ and $d^s = 0.267$, for $s = 2$.

The numerical solution of the first year is affected by the initial conditions, but during the successive years the solution is periodic without blow-ups nor damping effects (see Figure 6). Therefore, we run the model for five years and we compare the simulated adult population dynamics of the third year with the adult monitoring data.

In Figure 7.a the simulated adult population dynamics is compared with the adult monitoring data extracted from Salas-Araiza et al. (2018) referring to adult catches through a pheromone-baited trap located in Irapuato (Guanajuato, Mexico) in the year 2015.

In Figure 7.b the simulated adult population dynamics is compared with the adult monitoring data extracted from Garcia et al. (2018) referring to adult catches in Gainesville (Florida, US) in the year 2013.

From the numerical results shown in Figure 6 and Figure 7 we evince that the model proposed in this paper provides a reasonable interpretation of the main patterns related to the phenology and the abundance of the species.

The resulting values of the *root mean square error* are $RMSE \simeq 30.47$ for the calibration case (Guanajuato, Mexico) and $RMSE \simeq 194.94$ for the validation case (Gainesville, Florida, US).

Comparing population dynamics in simulation results with the validation dataset, we observe that the model capture the overall pattern of population dynamics in terms of level of abundance and the overall period of pest presence. However, there is a remarkable shift in the phenology described by the model that anticipates observations in the field. The model correctly describe the population reduction in the late seasons associated to unfavourable meteorological

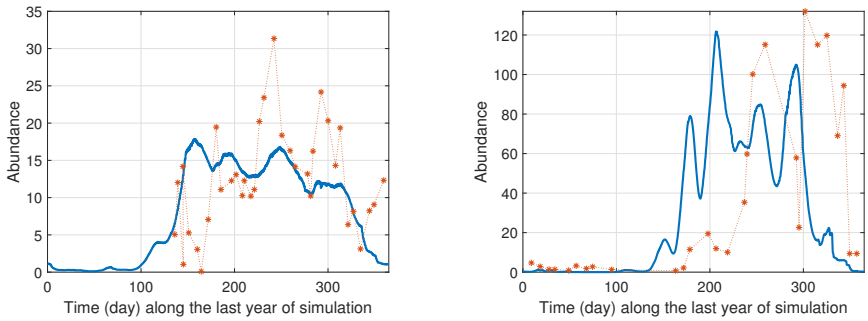

Figure 7: On the left: numerical solution for the stage $s = 4$ (continuous blue line) and experimental data (red asterisks) (Irapuato, Guanajuato, Mexico). On the right (Figure 7.b): numerical solution for the stage $s = 4$ (continuous blue line) and experimental data (red asterisks) (Gainesville, Florida, US). Parameters: $a^2 = 49.92$, $d^2 = 0.267$ and $a^s = d^s = 0$ for $s \neq 2$.

conditions (in the late autumn and winter).

If the density-dependent mortality term is nullified, we obtain a unlimited (and thus unrealistic) growth of the simulated population abundance. This is a confirmation that the regulation due to abiotic factors is not sufficient to model the population dynamics of the species. Although two extra parameters appear in the equation of our model, the benefits of our approach are considerable because the density dependent mortality term ensures a realistic limitation of the population abundance.

6. Conclusions and future perspectives

The model presented is characterised by a high degree of biological realism since it represents the temperature-dependent responses of the life-history strategies and it includes density-dependent control factors influencing the survival of the larval stage.

Our work mainly aims to explore the consequences of the introduction of a density-dependent control term in a stage-structured population dynamics model that is based on the Kolmogorov equation. We expect that the predictive performances of the model would improve by increasing the number of datasets used in the calibration procedure. In particular, it is important to estimate the model's parameters using datasets from different locations, thus allowing to investigate species' physiological responses to different environmental contexts. These aspects will be addressed in a subsequent work.

The mechanistic modelling approach we have used in our work allows to describe population dynamics in terms of variation of population abundance that is the main driver of the impact on host plants. This model output is particularly useful for supporting the implementation of knowledge-based management strategies of the pest species at various spatial-temporal scales. For instance, at the farm level, predictions on the time of emergence and the species' population

abundance can be exploited for planning and implementing pest monitoring and pest control activities (Rossi et al. (2019)). The model presented can also be applied at the regional level (e.g., at country or continental level) for the development of risk maps showing the potential distribution and abundance of the species under different climatic and risk management scenarios. These information are fundamental for guiding the categorization and prioritization of pest species and for assessing the potential risks of entry, establishment and impacts of the species (EFSA PLH Panel (2017), EFSA PLH Panel (2018a), EFSA PLH Panel (2018b), EFSA PLH Panel (2020)).

7. Appendix: Mathematical analysis of the model

We focus on Problem (P) stated by (17)–(20) in a single stage, omitting for simplicity the dependence on the stage s. In order to provide the analysis of the system in the more complex setting, we assume that the input flux $\mathcal{F}$ is defined as in (21), and the coefficients a and d appearing in the mortality term (15) are strictly positive.

Given the interval $(0,1)$ and a finite final time $T>0$, for every $t\in(0,T)$ we set

$$Q_t=(0,t)\times(0,1),\qquad Q=Q_T, \tag{54}$$

and denote for brevity

$$H=L^2(0,1),\qquad V=H^1(0,1),\qquad W=H^2(0,1), \tag{55}$$

with usual norms $\|\cdot\|_H$, $\|\cdot\|_V$ and $\|\cdot\|_W$. The symbols V' denotes the dual space of V, while the pair $\langle\cdot,\cdot\rangle_{V',V}$ represents the duality pairing between V' and V. Moreover, we identify H with its dual space. Now, we introduce the system under study. We assume

$$a,\ b,\ d\in(0,+\infty),\qquad F,\ S,\ M\in C^0([0,T]),\qquad F,\ S,\ M\geq 0, \tag{56}$$

$$G\in H,\qquad \varphi_0\in V,\qquad G,\ \varphi_0\geq 0. \tag{57}$$

We look for a function

$$\varphi\in H^1(0,T;V')\cap C^0([0,T];H)\cap L^2(0,T;V), \tag{58}$$

which solves Problem (P), namely

$$\partial_t\varphi(t,x)+\ \partial_x\Big(S(t)\varphi(t,x)-b\partial_x\varphi(t,x)\Big)$$

$$+\varphi(t,x)M(t)\left(1+a\left(\int_0^1\varphi(t,y)\ dy\right)^2\right)^d=0\qquad\text{in } Q_T, \tag{59}$$

$$\Big(S(t)\varphi(t,x)-b\ \partial_x\varphi(t,x)\Big)_{x=0}=F(t)\int_0^1 G(x)\varphi(t,x)\ dx, \tag{60}$$

$$\Big(- b\ \partial_x \varphi(t,x)\Big)_{x=1} = 0, \tag{61}$$

$$\varphi(0,x) = \varphi_0(x). \tag{62}$$

Omitting the dependence on the variable $x \in (0,1)$ in the integrand terms, we introduce the variational formulation of Problem (P), namely

$$S(t)\varphi(t,1)v(1) + \int_0^1 \partial_t\varphi(t)v\ dx + \int_0^1 \Big(b\partial_x\varphi(t) - S(t)\varphi(t)\Big)\partial_x v\ dx$$

$$+ \int_0^1 M(t)\varphi(t)\left(1 + a\left(\int_0^1 \varphi(t,y)\ dy\right)^2\right)^d v\ dx - F(t)v(0)\int_0^1 G\varphi(t)\ dx = 0,$$

$$\text{for a.e. } t \in (0,T) \text{ and for all } v \in V. \tag{63}$$

The following theorem is the main theoretical result of the paper, its proof will be developed in the next sections.

Theorem 7.1 (Well-posedness). *Assume* (56)–(57). *Then Problem* (P) *stated by* (59)–(62) *admits a unique solution* φ *satisfying* (58). *In particular, denoting by* $\varphi_{0,i}$, $i = 1,2$, *a pair of initial data and by* φ_i, $i = 1, 2$, *the corresponding solutions of Problem* (P), *the following continuous dependence estimate*

$$\|\varphi_1 - \varphi_2\|_{H^1(0,T;V')\cap C^0([0,T];H)\cap L^2(0,T;V)} \le c\|\varphi_{0,1} - \varphi_{0,2}\|_H \tag{64}$$

holds for some positive constant c *which depends only on the structure of our statement.*

We split the proof of this theorem in different steps.

7.1. Existence of solutions

7.1.1. The approximating Problem (P_τ)

In order to prove the existence of a solution to Problem (P) stated by (59)–(62), fix $N \in \mathbb{N}$ and consider a time delay $\tau = T/N$. Then, we look for a function

$$\varphi_\tau \in H^1(0,T;V') \cap C^0([0,T];H) \cap L^2(0,T;V), \tag{65}$$

satisfying the following approximating problem (P_τ), obtained by assuming a delay in the last term on the left hand side of (59), namely

$$\partial_t\varphi_\tau(t,x) + \ \partial_x\Big(S(t)\varphi_\tau(t,x) - b\partial_x\varphi_\tau(t,x)\Big)$$

$$+\varphi_\tau(t,x)M(t)\left(1 + a\left(\int_0^1 \varphi_\tau(t-\tau,y)\ dy\right)^2\right)^d = 0 \quad \text{in } Q_T, \tag{66}$$

$$\Big(S(t)\varphi_\tau(t,x) - b\ \partial_x\varphi_\tau(t,x)\Big)_{x=0} = F(t)\int_0^1 G(x)\varphi_\tau(t,x)\ dx, \tag{67}$$

$$\Big(- b\ \partial_x \varphi_\tau(t,x)\Big)_{x=1} = 0, \tag{68}$$

$$\varphi_\tau(t,x) = \varphi_0(x), \qquad \text{for every } t \le 0. \tag{69}$$

Omitting the dependence on the variable $x \in (0,1)$ in the integrand terms, we introduce the variational formulation of Problem (P_τ), namely

$$S(t)\varphi_\tau(t,1)v(1) + \int_0^1 \partial_t\varphi_\tau(t)v\ dx + \int_0^1 \Big(b\partial_x\varphi_\tau(t) - S(t)\varphi_\tau(t)\Big)\partial_x v\ dx$$

$$+ \int_0^1 M(t)\varphi_\tau(t)\left(1 + a\left(\int_0^1 \varphi_\tau(t-\tau,y)\ dy\right)^2\right)^d v\ dx$$

$$-F(t)v(0)\int_0^1 G\varphi_\tau(t)\ dx = 0 \qquad \text{for a.e. } t \in (0,T) \text{ and for all } v \in V. \tag{70}$$

Then, we can solve Problem (P_τ) stated by (66)–(69) in the interval $[0,\tau]$ (see, e.g., Dautray and Lions (1988), Sec. 3, Ch. XVIII), founding a solution

$$\varphi_\tau \in H^1(0,\tau;V') \cap C^0([0,\tau];H) \cap L^2(0,\tau;V). \tag{71}$$

Since $\varphi_\tau \in C^0([0,\tau];V)$, we can start again and get the solution of Problem (P_τ) in the interval $[\tau,2\tau]$. Repeating this explained technique, we can finally obtain a solution φ_τ of Problem (P_τ) (66)–(69) satisfying (65) and defined in the whole interval $[0,T]$.

7.1.2. A priori estimates on (P_τ)

In the remainder of the paper we often owe to the Hölder inequality and to the elementary Young inequalities in performing our a priori estimates. For every $x, y > 0$, $\alpha \in (0,1)$ and $\delta > 0$ there hold

$$xy \le \alpha x^{\frac{1}{\alpha}} + (1-\alpha)y^{\frac{1}{1-\alpha}}, \tag{72}$$

$$xy \le \delta x^2 + \frac{1}{4\delta}y^2. \tag{73}$$

Moreover, we also use the inequality deduced from the compactness of the embedding $V \subset H \subset V'$ (see Simon (1987), Lemma 8, p. 84): for all $\delta > 0$ there exists a constant $K > 0$ such that

$$\|z\|_H \le \delta\|z\|_V + K\|z\|_{V'} \qquad \text{for all } z \in H. \tag{74}$$

In the following, the symbol c stands for different positive constants which depend only on the final time T, on the shape of the nonlinearities and on the constants and the norms of the functions involved in the assumptions of our statements.

Testing (70) by φ_τ and integrating over $(0,t)$, we obtain

$$\frac{1}{2}\|\varphi_\tau(t)\|_H^2 + b\int_0^t\int_0^1 |\partial_x\varphi_\tau(s,x)|^2\ dx\ ds$$

$$+\frac{1}{2}\int_0^t S(s)|\varphi_\tau(s,1)|^2\ ds+\frac{1}{2}\int_0^t S(s)|\varphi_\tau(s,0)|^2\ ds$$

$$+\int_0^t\int_0^1 M(s)|\varphi_\tau(s,x)|^2\bigg(1+a\Big(\int_0^1\varphi_\tau(s-\tau,y)\ dy\Big)^2\bigg)^d\ dx\ ds$$

$$=\frac{1}{2}\|\varphi_0\|_H^2+\int_0^t F(s)\Big(\int_0^1 G(x)\varphi_\tau(s,x)\ dx\Big)\varphi_\tau(s,0)\ ds. \tag{75}$$

First of all, we observe that the last two terms on the left hand side of (75) is nonnegative, due to (56)–(57), while the first term on the right hand side is bounded thanks to (57). In order to estimate the second term on the right hand side of (75), we observe that

$$\varphi_\tau(s,0)=\varphi_\tau(s,x)-\int_0^x\partial_y\varphi_\tau(s,y)\ dy. \tag{76}$$

Then, integrating (76) over $(0,1)$, we have that

$$|\varphi_\tau(s,0)|\le\int_0^1|\varphi_\tau(s,x)|\ dx+\int_0^1\int_0^x|\partial_y\varphi_\tau(s,y)|\ dy\ dx, \tag{77}$$

and, using (72), we obtain that

$$|\varphi_\tau(s,0)|\le\|\varphi_\tau(s)\|_H+\|\partial_x\varphi_\tau(s)\|_H, \tag{78}$$

and, applying an analogous technique

$$|\varphi_\tau(s,1)|\le\|\varphi_\tau(s)\|_H+\|\partial_x\varphi_\tau(s)\|_H. \tag{79}$$

Finally, using (56)–(57) and (78), the last term on the right hand side of (75) can be estimated as follows:

$$\bigg|\int_0^t F(s)\Big(\int_0^1 G(x)\varphi_\tau(s,x)\ dx\Big)\varphi_\tau(s,0)\ ds\bigg|$$

$$\le\int_0^t|F(s)|\|G\|_H\|\varphi_\tau(s)\|_H\Big(\|\varphi_\tau(s)\|_H+\|\partial_x\varphi_\tau(s)\|_H\Big)\ ds$$

$$\le\|F\|_{C^0([0,T])}\|G\|_H\bigg(\int_0^t\|\varphi_\tau(s)\|_H^2\ ds+\int_0^t\|\varphi_\tau(s)\|_H\|\partial_x\varphi_\tau(s)\|_H\ ds\bigg)$$

$$\le c\int_0^t\|\varphi_\tau(s)\|_H^2\ ds+\frac{b}{2}\int_0^t\int_0^1|\partial_x\varphi_\tau(s,x)|^2\ dx\ ds. \tag{80}$$

Combining (75) with (80), we obtain that

$$\frac{1}{2}\|\varphi_\tau(t)\|_H^2+\frac{b}{2}\int_0^t\int_0^1|\partial_x\varphi_\tau(s,x)|^2\ dx\ ds+\frac{1}{2}\int_0^t S(s)|\varphi_\tau(s,1)|^2\ ds$$

$$+\int_0^t\int_0^1 M(s)|\varphi_\tau(s,x)|^2\biggl(1+a\Bigl(\int_0^1\varphi_\tau(s-\tau,y)\;dy\Bigr)^2\biggr)^d\;dx\;ds$$

$$+\frac12\int_0^t S(s)|\varphi_\tau(s,0)|^2\;ds\le c\biggl(1+\int_0^t\|\varphi_\tau(s)\|_V^2\;ds\biggr), \tag{81}$$

Applying the Gronwall lemma, we infer that

$$\frac12\|\varphi_\tau(t)\|_H^2+b\int_0^t\int_0^1|\partial_x\varphi_\tau(s,x)|^2\;dx\;ds$$

$$+\frac12\int_0^t S(s)|\varphi_\tau(s,1)|^2\;ds+\frac12\int_0^t S(s)|\varphi_\tau(s,0)|^2\;ds$$

$$+\int_0^t\int_0^1 M(s)|\varphi_\tau(s,x)|^2\biggl(1+a\Bigl(\int_0^1\varphi_\tau(s-\tau,y)\;dy\Bigr)^2\biggr)^d\;dx\;ds\le c, \tag{82}$$

whence we conclude that

$$\|\varphi_\tau\|_{C^0([0,T];H)\cap L^2(0,T;V)}\le c. \tag{83}$$

Now, we denote

$$I(t)=|M(t)|\biggl(1+a\Bigl(\int_0^1\varphi_\tau(t-\tau,x)\;dx\Bigr)^2\biggr)^d,\qquad \|I\|_{C^0([0,T])}\le c. \tag{84}$$

From (70), recalling that $V\subseteq L^\infty(0,1)$ with continuous embedding, (56)–(57) and (83)–(84) ensure that, for every $v\in L^2(0,T;V)$,

$$\biggl|\int_0^T\langle\partial_t\varphi_\tau(t),v(t)\rangle_{V,V'}\;dt\biggr|\le c\Bigl(\|\partial_x\varphi_\tau\|_{L^2(0,T;H)}+\|S\|_{C^0([0,T])}\|\varphi_\tau\|_{L^2(0,T;H)}$$

$$+\|S\|_{C^0([0,T])}\|\varphi_\tau\|_{L^2(0,T;V)}+2\|F\|_{C^0([0,T])}\|G\|_H\|\varphi_\tau\|_{L^2(0,T;H)} \tag{85}$$

$$+\|I\|_{C^0([0,T])}\|\varphi_\tau\|_{L^2(0,T;H)}\Bigr)\|v\|_{L^2(0,T;V)}\le c,$$

whence we obtain that

$$\|\partial_t\varphi_\tau\|_{L^2(0,T;V')}=\sup_{v\in L^2(0,T;V),\ \|v\|_{L^2(0,T;V)}=1}\biggl|\int_0^T\langle\partial_t\varphi_\tau(t),v(t)\rangle_{V,V'}\;dt\biggr|\le c,$$

which is equivalent to say that

$$\|\partial_t\varphi_\tau\|_{L^2(0,T;V')}\le c,\qquad\qquad \|\varphi_\tau\|_{H^1(0,T;V')}\le c. \tag{86}$$

7.1.3. Passage to the limit as $\tau \searrow 0$

Due to (83) and (86), Simon (1987)[Lemma 8, p. 84] (see also Colturato (2018), Colli and Colturato (2018)) ensures that there exists a subsequence $\tau_k \searrow 0$ such that, for every $\delta \in (0,1)$,

$$\varphi_{\tau_k} \longrightarrow \varphi \qquad \text{strongly in } L^2(0,T;H^{1-\delta}(0,1)), \tag{87}$$

which implies that

$$\varphi_{\tau_k}(\cdot,0) \longrightarrow \varphi(\cdot,0) \quad \text{strongly in } L^2(0,T), \tag{88}$$

$$\varphi_{\tau_k}(\cdot,1) \longrightarrow \varphi(\cdot,1) \quad \text{strongly in } L^2(0,T). \tag{89}$$

In particular, due to the properties of the translation function, from (88)–(89) we infer that

$$\varphi_{\tau_k}(\cdot-\tau_k,\cdot) \longrightarrow \varphi \qquad \text{strongly in } L^2(0,T;H^{1-\delta}(0,1)). \tag{90}$$

Then, we can pass to the limit as $\tau \searrow 0$ in (66)–(69) obtaining (59)–(62), whence we conclude that Problem (P) admits at least a solution satisfying (58).

7.2. Uniqueness and continuous dependence

Assume that a, b, d, S, M, F and G, are given as in (56)–(56) and let $\varphi_{0,i}$, $i=1,2$, be a pair of initial data. Denoting by φ_i, i = 1, 2, the corresponding solutions of Problem (P) (59)–(62) we set for brevity

$$J_i(s) = \left(1 + a\Big(\int_0^1 \varphi_i(s,y)\ dy\Big)^2\right)^d, \qquad i = 1,\ 2. \tag{91}$$

Then, we write Problem (P) for both φ_i, $i=1,2$ and take the difference between the respective equations. Denoting by $\varphi := \varphi_1 - \varphi_2$, we obtain that

$$\partial_t\varphi(t,x) + \ \partial_x\Big(S(t)\varphi(t,x) - b\partial_x\varphi(t,x)\Big)$$

$$+M(t)[\varphi_1(t,x)J_1(s) - \varphi_2(t,x)J_2(s)] = 0 \qquad \text{in } Q_T, \tag{92}$$

$$\Big(S(t)\varphi(t,x) - b\ \partial_x\varphi(t,x)\Big)_{x=0} = F(t)\int_0^1 G(y)\varphi(t,y)\ dy, \tag{93}$$

$$\Big(-b\ \partial_x\varphi(t,x)\Big)_{x=1} = 0, \tag{94}$$

$$\varphi(0,x) = 0. \tag{95}$$

We observe that, due to (58), there exists a positive constant C such that

$$\left|\int_0^1 \varphi_1(s,x)\ dx\right| + \left|\int_0^1 \varphi_2(s,x)\ dx\right| \le C, \qquad \text{for every } s \in [0,T]. \tag{96}$$

Since the real function $R : \ r \longmapsto (1+ar^2)^d$ is Lipschitz continuous in the interval $[-C, C]$, we infer that

$$\begin{aligned} |J_1(s) - J_2(s)| &\leq L\left| \int_0^1 \varphi_1(s,x)\ dx - \int_0^1 \varphi_2(s,x)\ dx \right| \\ &\leq L\int_0^1 |\varphi_1(s,x) - \varphi_2(s,x)|\ dx \\ &= L\int_0^1 |\varphi(s,x)|\ dx \leq L\|\varphi(s)\|_H, \end{aligned} \tag{97}$$

for every $s \in [0,T]$, where L is the Lipschitz constant of the function R. Testing (92) by φ and integrating over Q_t, we obtain that

$$\begin{aligned} &\frac{1}{2}\|\varphi(t)\|_H^2 + b\int_{Q_t} |\partial_x\varphi_\tau(s,x)|^2\ dx\ ds \\ &+\frac{1}{2}\int_0^t S(s)|\varphi_\tau(s,1)|^2\ ds + \frac{1}{2}\int_0^t S(s)|\varphi_\tau(s,0)|^2\ ds \\ &= -\int_{Q_t} M(s)[\varphi_1(s,y)J_1(s) - \varphi_2(s,y)J_2(s)]\varphi(s,y)\ dy\ ds \\ &+\int_0^t F(s)\varphi(s,0)\left(\int_0^1 G(y)\varphi(s,y)\ dy\right) ds + \frac{1}{2}\|\varphi_{0,1} - \varphi_{0,2}\|_H^2. \end{aligned} \tag{98}$$

We observe that the first term on the right hand side of (98) can be rewritten as

$$\begin{aligned} &-\int_{Q_t} M(s)[\varphi_1(s,x)J_1(s) - \varphi_2(s,x)J_2(s)]\varphi(s,x)\ dx\ ds \\ &= -\int_{Q_t} M(s)[(\varphi_1(s,x) - \varphi_2(s,x))J_1(s) + \varphi_2(s,x)(J_1(s) - J_2(s))]\varphi(s,x)\ dx\ ds \\ &= -\int_{Q_t} M(s)|\varphi(s,x)|^2 J_1(s)\ dx\ ds - \int_{Q_t} M(s)\varphi_2(s,x)[J_1(s) - J_2(s)]\varphi(s,x)\ dx\ ds. \end{aligned} \tag{99}$$

Then, moving to the left hand side of (98) the nonnegative term

$$\int_{Q_t} M(s)|\varphi(s,x)|^2 J_1(s)\ dx\ ds,$$

we have only to estimate the last term of (99) using (56)–(57) and (97), namely

$$\begin{aligned} &-\int_{Q_t} M(s)\varphi_2(s,x)(J_1(s) - J_2(s))\varphi(s,x)\ dx\ ds \\ &\leq \|M\|_{C^0([0,T])}\|\varphi_2\|_{C^0([0,T];H)}\int_0^t |J_1(s) - J_2(s)|\|\varphi(s)\|_H\ ds \end{aligned}$$

$$\leq L\|M\|_{C^0([0,T])}\|\varphi_2\|_{C^0([0,T];H)}\int_0^t \|\varphi(s)\|_H^2\ ds$$
$$\leq c\int_0^t \|\varphi(s)\|_H^2\ ds. \tag{100}$$

In order to estimate the second term on the right hand side of (98), we observe that

$$\varphi(s,0) = \varphi(s,x) - \int_0^x \partial_y\varphi(s,y)\ dy. \tag{101}$$

Integrating (101) over $(0,1)$, we have that

$$\begin{aligned} |\varphi(s,0)| &\leq \int_0^1 |\varphi(s,x)|\ dx + \int_0^1\int_0^x |\partial_y\varphi(s,y)|\ dy\ dx \\ &\leq \int_0^1 |\varphi(s,x)|\ dx + \int_0^1\int_0^1 |\partial_y\varphi(s,y)|\ dy\ dx, \end{aligned} \tag{102}$$

whence, using (72), we infer that

$$|\varphi(s,0)| \leq \|\varphi(s)\|_H + \|\partial_x\varphi(s)\|_H. \tag{103}$$

Consequently, due to (56)–(57) and (103), the last term on the right hand side of (98) can be estimated as follows:

$$\left|\int_0^t F(s)\varphi(s,0)\Big(\int_0^1 G(x)\varphi(s,x)\ dx\Big)\ ds\right|$$
$$\leq \int_0^t |F(s)|\|G\|_H\|\varphi(s)\|_H\Big(\|\varphi(s)\|_H + \|\partial_x\varphi(s)\|_H\Big)\ ds$$
$$\leq \|F\|_{C^0([0,T])}\|G\|_H\Big(\int_0^t \|\varphi(s)\|_H^2\ ds + \int_0^t \|\varphi(s)\|_H\|\partial_x\varphi(s)\|_H\ ds\Big)$$
$$\leq \frac{1}{2}\|\varphi_{0,1}-\varphi_{0,2}\|_H^2 + c\int_0^t \|\varphi(s)\|_H^2\ ds + \frac{b}{2}\int_{Q_t} |\partial_x\varphi(s,x)|^2\ dx\ ds. \tag{104}$$

Combining (98) with (100) and (104), we obtain that

$$\frac{1}{2}\|\varphi(t)\|_H^2 + \frac{b}{2}\int_{Q_t} |\partial_x\varphi_\tau(s,x)|^2\ dx\ ds + \frac{1}{2}\int_0^t S(s)|\varphi_\tau(s,1)|^2\ ds$$
$$+\frac{1}{2}\int_0^t S(s)|\varphi_\tau(s,0)|^2\ ds \leq c\int_0^t \|\varphi(s)\|_H^2\ ds. \tag{105}$$

Applying the Gronwall lemma, we infer that

$$\frac{1}{2}\|\varphi(t)\|_H^2 + \frac{b}{2}\int_{Q_t} |\partial_x\varphi_\tau(s,x)|^2\ dx\ ds + \frac{1}{2}\int_0^t S(s)|\varphi_\tau(s,1)|^2\ ds \tag{106}$$
$$+\frac{1}{2}\int_0^t S(s)|\varphi_\tau(s,0)|^2\ ds \leq c\|\varphi_{0,1}-\varphi_{0,2}\|_H^2, \tag{107}$$

whence the continuous dependence estimate (64) is proved. In particular, if $\varphi_{0,1} = \varphi_{0,2}$, then (107) ensures that the solution of Problem (P) is unique.

Acknowledgements

The authors kindly thank Dr. Allan J. Hruska (Food and Agriculture Organization of the United Nations) and Assistant Professor Robert L. Meagher (United States Department of Agriculture - Agricultural Research Service) for sharing their knowledge on the biology and the ecology of the fall armyworm and the protocols applied for its management.

The authors gratefully acknowledge the GNAMPA (Gruppo Nazionale per l'Analisi Matematica, la Probabilità e le loro Applicazioni) and the GNCS (Gruppo Nazionale per il Calcolo Scientifico) of INdAM (Istituto Nazionale di Alta Matematica).

Conflict of interest

The authors declare that they have no conflict of interest.

References

Abia, L., Angulo, O., López-Marcos, J., 2004. Size-structured population dynamics models and their numerical solutions. Discrete and Continuous Dynamical Systems - Series B 4, 1203–1222.

Allen, E., 2009. Derivation of stochastic partial differential equations for size- and age-structured populations. Journal of Biological Dynamics 3, 73–86.

Andow, D., Farias, J., Horikoshi, R., Bernardi, D., Nascimento, A., Omoto, C., 2015. Dynamics of cannibalism in equal-aged cohorts of Spodoptera frugiperda. Ecological Entomology 40, 229–236.

Angulo, O., López-Marcos, J., 2004. Numerical integration of fully nonlinear size-structured population models. Applied Numerical Mathematics 50, 291–327.

Barfield, C.S., Mitchell, E.R., Poeb, S.L., 1978. A Temperature-Dependent Model for Fall Armyworm Development1,2. Annals of the Entomological Society of America 71, 70–74.

Barros, E., Torres, J., Bueno, A., 2010a. Oviposition, development, and reproduction of Spodoptera frugiperda (J.E. Smith) (Lepidoptera: Noctuidae) fed on different hosts of economic importance [oviposição, desenvolvimento e reprodução de Spodoptera frugiperda (J.E. Smith) (Lepidoptera: Noctuidae) em diferentes hospedeiros de importância econômica]. Neotropical Entomology 39, 996–1001.

Barros, E.M., Torres, J.B., Bueno, A.F., 2010b. Oviposicao, desenvolvimento e reproducao de Spodoptera frugiperda (lepidoptera: Noctuidae) diferentes hospedeiros de importancia economica. Neotropical Entomology 39, 996–1001.

Batchelder, H., Edwards, C., Powell, T., 2002. Individual-based models of copepod populations in coastal upwelling regions: Implications of physiologically and environmentally influenced diel vertical migration on demographic success and nearshore retention. Progress in Oceanography 53, 307–333.

Baudron, F., Zaman-Allah, M., Chaipa, I., Chari, N., Chinwada, P., 2019. Understanding the factors influencing fall armyworm (Spodoptera frugiperda j.e. smith) damage in african smallholder maize fields and quantifying its impact on yield. a case study in eastern zimbabwe. Crop Protection 120, 141–150.

Bergh, M., Getz, W., 1988. Stability of discrete age-structured and aggregated delay-difference population models. Journal of Mathematical Biology 26, 551–581.

Briere, J.F., Pracros P., Le Roux, A.Y., Pierre, J.S., 1999. A novel rate model oftemperature-dependent development for arthropods. Environ. Entomol. 28, 22–29.

Buffoni, G., Cappelletti, A., 2000. Size structured populations: Dispersion effects due to stochastic variability of the individual growth rate. Mathematical and Computer Modelling 31, 27–34.

Buffoni, G., Pasquali, S., 2007. Structured population dynamics: Continuous size and discontinuous stage structures. Journal of Mathematical Biology 54, 555–595. doi:10.1007/s00285-006-0058-2.

Buffoni, G., Pasquali, S., 2010. Individual-based models for stage structured populations: Formulation of "no regression" development equations. Journal of Mathematical Biology 60, 831–848.

Buffoni, G., Pasquali, S., Gilioli, G., 2004. A stochastic model for the dynamics of a stage structured population. Discrete and Continuous Dynamical Systems - Series B 4, 517–525.

Busato, G., Grützmacher, A., Garcia, M., Giolo, F., Zotti, M., Bandeira, J., 2005. Thermal requirements and estimate of the number of generations of biotypes "corn" and "rice" of Spodoptera frugiperda [exigências térmicas e estimativa do número de gerações dos biótipos "milho" e "arroz" de Spodoptera frugiperda]. Pesquisa Agropecuaria Brasileira 40, 329–335.

Charles, H., Dukes, J.S., 2014. Impacts of invasive species on ecosystem services. Springer, Berlin, Heidelberg.

Clother, D., Brindley, J., 2000. Stochastic development of individual members of a population: A brownian motion approach. Bulletin of Mathematical Biology 62, 1003–1034.

Colli, P., Colturato, M., 2018. Global existence for a singular phase field system related to a sliding mode control problem. Nonlinear Analysis: Real World Applications 41, 128–151.

Colturato, M., 2018. On a class of conserved phase field systems with a maximal monotone perturbation. Applied Mathematics and Optimization 78, 545–585.

Cushing, J., 1992. A discrete model for competing stage-structured species. Theoretical Population Biology 41, 372–387.

Dautray, R., Lions, J., 1988. Analyse mathématique et calcul numérique pour les sciences et les techniques (VIII). Masson, Paris.

Dautray, R., Lions, J., 1992. Mathematical analysis and numerical methods for science and technology (V). Springer, New York.

Day, R., Abrahams, P., Bateman, M., Beale, T., Clottey, V., Cock, M., Colmenarez, Y., Corniani, N., Early, R., Godwin, J., Gomez, J., Moreno, P., Murphy, S., Oppong-Mensah, B., Phiri, N., Pratt, C., Silvestri, S., Witt, A., 2017. Fall armyworm: Impacts and implications for africa. Outlooks on Pest Management 28, 196–201.

Deangelis, D., Cox, D., Coutant, C., 1980. Cannibalism and size dispersal in young-of-the-year largemouth bass: Experiment and model. Ecological Modelling 8, 133–148.

Di Cola, G., Buffoni, G., Ugolini, A., 1990. Discrete Stochastic Models in Population Dynamics with Physiological Age Structure. Technical Report 57. Quaderni del Dipartimento di Matematica dell'Università di Parma.

Diekmann, O., Gyllenberg, M., Huang, H., Kirkilionis, M., Metz, J., Thieme, H., 2001. On the formulation and analysis of general deterministic structured population models: Ii. nonlinear theory. Journal of Mathematical Biology 43, 157–189.

Early, R., González-Moreno, P., Murphy, S., Day, R., 2018. Forecasting the global extent of invasion of the cereal pest Spodoptera frugiperda, the fall armyworm. NeoBiota , 25–50.

EFSA PLH Panel (2017), 2017. (EFSA Panel on Plant Health). Scientific opinion on the pest risk assessment of Spodoptera frugiperda. EFSA Journal 15, 1–32. doi:https://doi.org/10.2903/j.efsa.2017.4927.

EFSA PLH Panel (2018a), 2018. (EFSA Panel on Plant Health). Scientific opinion on the pest risk assessment of Spodoptera frugiperda for the European Union. EFSA Journal 16, 1–120. doi:https://doi.org/10.2903/j.efsa.2018.5351.

EFSA PLH Panel (2018b), 2018. (EFSA Panel on Plant Health). Guidance on quantitative pest risk assessment. EFSA Journal 16, 996–1001.

EFSA PLH Panel (2020), 2020. (EFSA Panel on Plant Health). Pest survey card on Spodoptera frugiperda. EFSA supporting publication 2020:EN-1895 16, 1–29. doi:10.2903/sp.efsa.2020.EN-1895.

FAO, 2018. Briefing Note on FAO Actions on Fall Armyworm in Africa. Technical Report.

FAO, 2019a. First detection of fall armyworm in bangladesh. FAO Official Pest Report c, https://www.ippc.int/fr/news/first–detection–of–fall–armyworm–in–bangladesh/.

FAO, 2019b. First detection of fall armyworm in china. FAO Official Pest Report b, https://www.ippc.int/fr/news/first–detection–of–fall–armyworm–in–china/.

FAO, 2019c. First detection report of the fall armyworm Spodoptera frugiperda (lepidoptra: Noctuidae) on maize in myanmar. IPPC Official Pest Report 1, https://www.ippc.int/en/.

FAO, 2019d. Statement on fall armyworm in sri lanka. FAO Official Pest Report a.

FAO, 2020. Detection of fall armyworm. FAO Official Pest Report .

Farias, P., Barbosa, J., Busoli, A., Overal, W., Miranda, V., Ribeiro, S., 2008. Spatial analysis of the distribution of Spodoptera frugiperda (j.e. smith) (lepidoptera: Noctuidae) and losses in maize crop productivity using geostatistics. Neotropical Entomology 37, 321–327.

Ganiger, P., Yeshwanth, H., Muralimohan, K., Vinay, N., Kumar, A., Chandrashekara, K., 2018. Occurrence of the new invasive pest, fall armyworm, Spodoptera frugiperda (j.e. smith) (lepidoptera: Noctuidae), in the maize fields of karnataka, india. Current Science 115, 621–623.

Garcia, A., Ferreira, C., Godoy, W., Meagher, R., 2019. A computational model to predict the population dynamics of Spodoptera frugiperda. Journal of Pest Science 92, 429–441.

Garcia, A., Godoy, W., Thomas, J., Nagoshi, R., Meagher, R., 2018. Delimiting strategic zones for the development of fall armyworm (lepidoptera: Noctuidae) on corn in the state of florida. Journal of Economic Entomology 111, 120–126.

Gilioli, G., Pasquali, S., 2007. Use of individual-based models for population parameters estimation. Ecological modelling 200, 109–118.

Gilioli, G., Pasquali, S., Marchesini, E., 2016. A modelling framework for pest population dynamics and management: An application to the grape berry moth. Ecological Modelling 320, 348–357.

Gilioli, G., Pasquali, S., Parisi, S., Winter, S., 2014. Modelling the potential distribution of Bemisia tabaci in Europe in light of the climate change scenario. Pest Management Science 70, 1611–1623.

Goergen, G., Kumar, P., Sankung, S., Togola, A., Tamò, M., 2016. First report of outbreaks of the fall armyworm Spodoptera frugiperda (j e smith) (lepidoptera, noctuidae), a new alien invasive pest in west and central africa. PLoS ONE 11.

Gurtin, M., Maccamy, R., 1974. Non-linear age-dependent population dynamics. Archive for Rational Mechanics and Analysis 54, 281–300.

Gutierrez, A.P., 1996. Applied population ecology: a supply-demand approach. John Wiley & Sons.

Gyllenberg, M., Hanski, I., 1992. Single-species metapopulation dynamics: A structured model. Theoretical Population Biology 42, 35–61.

Gyori, I., 1990. Some mathematical aspects of modelling cell population dynamics. Computers and Mathematics with Applications 20, 127–138.

Hogg, D.B., Pitre, H.N., Anderson, R.E., 1982. Assessment of Early-Season Phenology of the Fall Armyworm (Lepidoptera: Noctuidae) in Mississippi 1. Environmental Entomology 11, 705–710.

Huffaker, C., Gutierrez, A., 1999. Ecological Entomology. Wiley, New York.

Iannelli, M., 1994. Mathematical theory of age-structured population dynamics. Giardini, Pisa.

IPPC, 2018. First detection of fall army worm on the border of thailand. IPPC Official Pest Report 1, https://www.ippc.int/.

IPPC, 2019. Report of first detection of fall armyworm in republic of korea. IPPC Official Pest Report , https://www.ippc.int/.

Kelpin, F., Kirkilionis, M., Kooi, B., 2000. Numerical methods and parameter estimation of a structured population model with discrete events in the life history. Journal of Theoretical Biology 207, 217–230.

Kumela, T., Simiyu, J., Sisay, B., Likhayo, P., Mendesil, E., Gohole, L., Tefera, T., 2019. Farmers' knowledge, perceptions, and management practices of the new invasive pest, fall armyworm (Spodoptera frugiperda) in ethiopia and kenya. International Journal of Pest Management 65, 1–9.

Lee, K., Barr, R., Gage, S., Kharkar, A., 1976. Formulation of a mathematical model for insect pest ecosystems-the cereal leaf beetle problem. Journal of Theoretical Biology 59, 33–76.

LeVeque, R.J., 2002. Finite volume methods for hyperbolic problems. Cambridge University Press, Cambridge.

Liu, T., Wang, J., Hu, X., Feng, J., 2020. Land-use change drives present and future distributions of fall armyworm, Spodoptera frugiperda (j.e. smith) (lepidoptera: Noctuidae). Science of the Total Environment 706.

Mazza, G., Tricarico, E., Genovesi, P., Gherardi, F., 2014. Biological invaders are threats to human health: An overview. Ethology Ecology and Evolution 26, 112–129.

Mazzocchi, M., Buffoni, G., Carotenuto, Y., Pasquali, S., Ribera d'Alcalà, M., 2006. Effects of food conditions on the development of the population of temora stylifera: A modeling approach. Journal of Marine Systems 62, 71–84.

Milano, P., Berti Filho, E., Parra, J., Cônsoli, F., 2008. Temperature effects on the mating frequency of anticarsia gemmatalis hüebner and Spodoptera frugiperda (j.e. smith) (lepidoptera: Noctuidae) [influência da temperatura na freqüência de cópula de anticarsia gemmatalis hübner e Spodoptera frugiperda (j.e. smith) (lepidoptera: Noctuidae)]. Neotropical Entomology 37, 528–535.

Murúa, G., Virla, E., 2004. Population parameters of Spodoptera frugiperda (Smith) (Lep.: Noctuidae) fed on corn and two predominant grasess in Tucuman (Argentina). Acta zoológica mexicana 20, 199 – 210.

Oeh, U., Dyker, H., LÖSel, P., Hoffmann, K., 2001. In vivo effects of manduca sexta allatotropin and allatostatin on development and reproduction in the fall armyworm, Spodoptera frugiperda (lepidoptera, noctuidae). Invertebrate Reproduction and Development 39, 239–247.

Paini, D., Sheppard, A., Cook, D., De Barro, P., Worner, S., Thomas, M., 2016. Global threat to agriculture from invasive species. Proceedings of the National Academy of Sciences of the United States of America 113, 7575–7579.

Pashley, D.P., Hardy, T.N., Hammond, A.M., 1995. Host effects on developmental and reproductive traits in fall armyworm strains (Lepidoptera: Noctuidae). Annals of the Entomological Society of America 88, 748–755.

Pasquali, S., Mariani, L., Calvitti, M., Moretti, R., Ponti, L., Chiari, M., Sperandio, G., Gilioli, G., 2020. Development and calibration of a model for the potential establishment and impact of aedes albopictus in europe. Acta tropica 202, 105–228.

Plant, R., Wilson, L., 1986. Models for age structured populations with distributed maturation rates. Journal of Mathematical Biology 23, 247–262.

Pólik, I., Terlaky, T., 2010. Interior Point Methods for Nonlinear Optimization. Springer. volume 1989 of *Lecture Notes in Mathematics*. pp. 215–276. Lectures given at the C.I.M.E. Summer School held in Cetraro, July 2007. Edited by G. Di Pillo and F. Schoen.

Ponosov, A., Idels, L., Kadiev, R., 2020. Stochastic mckendrick–von foerster models with applications. Physica A: Statistical Mechanics and its Applications 537.

Ponti, L., Gilioli, G., Biondi, A., Desneux, N., Gutierrez, A., 2015. Physiologically based demographic models streamline identification and collection of data in evidence-based pest risk assessment. EPPO Bulletin 45, 317–322.

Prasanna, B.M., Huesing, J.E., Eddy, R., Peschke, V.M., 2018. Fall armyworm in Africa: a guide for integrated pest management. Technical Report.

Quarteroni, A., 2017. Numerical Models for Differential Problems, 3rd ed. Springer International Publishing.

Quarteroni, A., Saleri, F., Gervasio, P., 2014. Scientific Computing with MATLAB and Octave 4th ed. Springer-Verlag, Berlin Heidelberg.

Regniere, J., Powell, J., Bentz, B., Nealis, V., 2012. Effects of temperature on development, survival and reproduction of insects: Experimental design, data analysis and modeling. Journal of Insect Physiology 58, 634–647.

Rios, E.S., Martins, I., de Noronha, M.P., de Silva, A., da Silva Filho, J., Badji, C., 2014a. Spatial distribution of Spodoptera frugiperda in the wasteland of southern pernambuco state, brazil. Revista de Ciências Agrarias - Amazon Journal of Agricultural and Environmental Sciences 57, 297–304. doi:10.4322/rca.ao1461.

Rios, E.S., Martins, I.C.F., Noronha, M.P., Silva, J.A., Silva Filho, J.G., Badji, C.A., 2014b. Spatial distribution of Spodoptera frugiperda in the wasteland of southern pernambuco state. Revista de Ciencias Agrarias Amazonian Journal of Agricultural and Environmental Sciences 57, 297–304.

Robertson, S., Henson, S., Robertson, T., Cushing, J., 2018. A matter of maturity: To delay or not to delay? continuous-time compartmental models of structured populations in the literature 2000–2016. Natural Resource Modeling 31.

Ros-Dez, J., Saldamando-Benjumea, C., 2011. Susceptibility of Spodoptera frugiperda (lepidoptera: Noctuidae) strains from central colombia to two insecticides, methomyl and lambda-cyhalothrin: A study of the genetic basis of resistance. Journal of Economic Entomology 104, 1698–1705.

Rossi, V., Sperandio, G., Caffi, T., Simonetto, A., Gilioli, G., 2019. Critical success factors for the adoption of decision tools in ipm. Agronomy 9, 103–121.

Royer, T.A., Edelson, J.V., Harris, M.K., 1999. Temperature related, stage-specific development and fecundity of colonizing and root-feeding morphs of pemphigus populitransversus (homoptera: Aphididae) on brassica. Environ. Entomol. 28, 265–271.

Salas-Araiza, M.D., Martínez-Jaime, O.A., Guzmán-Mendoza, R., González-Márquez, M., Ávila-López, Á., 2018. Fluctuación poblacional de Spodoptera frugiperda (je smith) y Spodoptera exigua (hubner)(lepidoptera: Noctuidae) mediante el uso de feromonas en iraputo. Gto. Mex. Entomol. Mex 5, 368–374.

Simmons, A.M., 1993. Effects of constant and fluctuating temperatures and humidities on the survival of Spodoptera frugiperda pupae (lepidoptera: Noctuidae). The Florida Entomologist 76, 333–340.

Simon, J., 1987. Compact sets in the spaces $l^p(0,t;b)$. Ann. Mat. Pura. Appl 146, 65–96.

Sinclair, A., Pech, R., 1996. Density dependence, stochasticity, compensation and predator regulation. Oikos 75, 164–173.

Sporleder, M., Kroschel, J., Gutierrez Quispe, M., Lagnaoui, A., 2004. A temperature-based simulation model for the potato tuberworm, phthorimaea operculella zeller (lepidoptera; gelechiidae). Environmental Entomology 33, 477–486.

Tamburini, G., Marini, L., Hellrigl, K., Salvadori, C., Battisti, A., 2013. Effects of climate and density-dependent factors on population dynamics of the pine processionary moth in the southern alps. Climatic Change 121, 701–712.

Valdez-Torres, J., Soto-Landeros, F., Osuna-Enciso, T., Báez-Sañudo, M., 2012. Phenological prediction models for white corn (zea mays l.) and fall armyworm (Spodoptera frugiperda j.e. smith) [modelos de predicción fenológica para maíz blanco (zea mays l.) y gusano cogollero (Spodoptera frugiperda j. e. smith)]. Agrociencia 46, 399–410.

Varella, A., Menezes-Netto, A., De Souza Alonso, J., Caixeta, D., Peterson, R., Fernandes, O., 2015. Mortality dynamics of Spodoptera frugiperda (lepidoptera: Noctuidae) immatures in maize. PLoS ONE 10.

Wagner, T.L., Wu, H.I., Sharpe, P., Schoolfield, R.M., Coulson, R.N., 1984. Modeling insect development rates: a literature review and application ofa biophysical model. Ann. Entomol. Soc. Am. 77, 208–225.

Wang, R., Jiang, C., Guo, X., Chen, D., You, C., Zhang, Y., Wang, M., Li, Q., 2020. Potential distribution of Spodoptera frugiperda (j.e. smith) in china and the major factors influencing distribution. Global Ecology and Conservation 21.